



## Post-Buckling, Strength and Design of Cold-Formed Steel Lipped Channel, Hat-Section and Zed-Section Columns Affected by Local-Distortional Interaction

P.B. Dinis<sup>1</sup>, D. Camotim<sup>1</sup>, R. Fena<sup>1</sup>

### Abstract

This work reports the latest results of an ongoing investigation on the post-buckling behavior, strength and design of cold-formed steel columns affected by local-distortional interaction, aimed at extending findings recently obtained for lipped channels to other cross-section shapes. Initially, the paper compares the elastic and elastic-plastic post-buckling and strength behaviors of hat-section, zed-section and lipped channel fixed-ended columns sharing cross-section dimensions (web, flange and lip widths) and lengths that lead to virtually identical local and distortional buckling loads, *i.e.*, to a high susceptibility to local-distortional mode interaction – note that the three columns exhibit the same local and distortional buckling behaviors. Then, the paper presents and discusses the results of an extensive parametric study, carried out by means of ABAQUS shell finite element analyses, aimed at determining the “exact” ultimate loads of 210 pairs of initially imperfect hat-section and zed-section columns with various geometries, all of them associated with strong local-distortional interaction – the cross-section dimensions and lengths of these column pairs are those exhibited by fixed-ended lipped channel columns that were analyzed in previous investigations. Finally, the ultimate strength data gathered are used to assess the performance of a recent design approach, based on the Direct Strength Method (DSM) and developed/validated in the context of cold-formed steel fixed-ended lipped channel columns undergoing local-distortional interaction, in order to assess whether it can be successfully applied to hat and zed-section columns under the same conditions.

### 1. Introduction

Cold-formed steel members invariably display slender thin-walled open cross-sections, which makes highly prone to instability phenomena involving cross-section deformation, namely local and distortional buckling – Fig. 1 shows hat-section column cross-section buckled shapes corresponding to local, distortional and global (flexural-torsional and flexural) modes. Moreover, several commonly used member geometries (unrestrained length and cross-section shape/dimensions) are associated with similar local and distortional buckling stresses, which automatically implies that the corresponding post-buckling behaviors (elastic or elastic-plastic), ultimate strength and failure mechanism are influenced by the coupling effects between these two buckling modes. Indeed, this influence has already been well studied, characterized and quantified, both numerically and experimentally, for lipped channel columns (mostly) and beams (Dinis *et al.* 2007, 2009a, Young *et al.* 2009, 2012 and Dinis & Camotim 2010).

<sup>1</sup> Department of Civil Engineering, ICIST, Instituto Superior Técnico, Technical University of Lisbon, Portugal.  
<[dinis@civil.ist.utl.pt](mailto:dinis@civil.ist.utl.pt)>, <[dcamotim@civil.ist.utl.pt](mailto:dcamotim@civil.ist.utl.pt)> and <[rufena@gmail.com](mailto:rufena@gmail.com)>

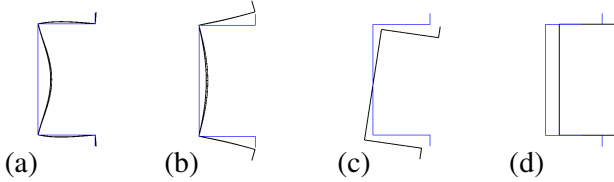


Figure 1: Hat-section column cross-section buckled shapes corresponding to (a) local, (b) distortional, (c) flexural-torsional and (d) flexural buckling modes

Since the structural behavior and strength of cold-formed steel members is complex and often not yet adequately reflected in most current design codes, a considerable amount of research work has been devoted to the development of efficient (safe and economic) design rules for such members. Undoubtedly the most relevant fruit of this intense research activity was the “Direct Strength Method” (DSM), which (i) has its roots in the work of Hancock *et al.* (1994), (ii) was originally proposed by Schafer & Peköz (1998) and (iii) has been continuously improved, mostly due to Schafer’s efforts (*e.g.*, Schafer 2008). The DSM (i) is currently capable of predicting the strength of columns and beams failing in local, distortional, global and local-global interactive modes, (ii) does not require any “effective width” calculations and (iii) has already been incorporated in the current versions of the North American (AISI 2007) and Australian/New Zealand (AS/NZS 2005) cold-formed steel specifications. However, as pointed out by Schafer (2008), further research is needed before the DSM approach can be applied to members affected by mode interaction phenomena involving distortional buckling. In the particular case of lipped channel columns (either pin-ended or fixed-ended) exhibiting local-distortional interaction, the first two authors have already conducted extensive numerical simulations that (i) provided clear evidence that the currently DSM local and distortional design curves cannot capture adequately the ultimate strength erosion stemming from interactive behavior and also (ii) enabled them to unveil key features that must appear in a novel DSM approach for such members – they were incorporated into proposals/guidelines for the development of a new DSM strength curve (Camotim *et al.* 2008, Silvestre *et al.* 2009, 2012, Young *et al.* 2012). Moreover, the experimental results obtained from the column tests reported by Yang & Hancock (2004), Kwon *et al.* (2009), Young *et al.* (2009, 2012) and Yap & Hancock (2011) also confirmed the ultimate strength erosion due to local-distortional interaction.

The aim of this work is to extend the previous investigations carried out by the first two authors, in the context of fixed-ended cold-formed steel ( $E=210\text{GPa}$ ,  $\nu=0.3$ ) lipped channel columns (Dinis *et al.* 2009a), to hat and zed-section columns equally affected by strong local-distortional interaction – note that (i) columns with these three cross-sections (and the same dimensions) exhibit practically identical local and distortional buckling behaviors and (ii) some results concerning hat-section columns have already been reported (Dinis *et al.* 2011). The first part of the paper compares the (i) post-buckling behavior (elastic and elastic-plastic), (ii) ultimate strength and (iii) failure mode nature of the three column families under consideration – as logically anticipated, the identical cross-section dimensions and lengths, identified by means of trial-and error buckling analyses performed for the lipped channel columns (Silvestre *et al.* 2009, 2012), lead to virtually coincident local (L) and distortional (D) buckling loads for each column trio. The results presented and discussed concern a large number of hat and zed-section columns differing only in the initial geometrical imperfection shape. The various imperfection shapes dealt with consist of different linear combinations of the competing L and D critical buckling mode shapes, all of them sharing a common amplitude equal to 10% of the wall thickness  $t$ , and a relevant outcome of this study is the identification of the most detrimental imperfection shapes, in the sense that they lead to lower column strengths. Next, the paper presents and discusses the results of a extensive parametric study, carried out by means of ABAQUS (Simulia 2008) shell finite element analyses (as all the numerical post-buckling results

reported in this work)<sup>2</sup>, aimed at obtaining “exact” ultimate loads for 210 pairs of fixed-ended hat and zed-section columns (i) with various geometries associated with strong local-distortional interaction (previously selected in the context of fixed-ended lipped channel columns – Silvestre *et al.* 2009, 2012) and (ii) containing the most detrimental initial imperfection shapes. Finally, the ultimate strength data gathered in the above parametric study are used to assess the performance of a novel DSM-based design approach that (i) is specifically intended to estimate column ultimate strengths corresponding to local-distortional interactive failures, stemming from nearly coincident local and distortional critical buckling loads<sup>3</sup>, and (ii) was recently developed and validated in the context of lipped channel columns (Silvestre *et al.* 2012) – this approach adopts Winter-type curves and is based on the values of (i) the elastic critical (local and distortional) buckling stress, (ii) the critical half-wave length ratio  $L_{crD}/L_{crL}$  and (iii) the cross-section elastic/plastic capacity. The aim is to find out whether the above novel DSM-based design approach can be successfully applied to hat and zed-section columns under the same circumstances.

## 2. Local-Distortional Buckling Mode Interaction

This section presents and discusses the main results of an investigation on the buckling, post-buckling (elastic and elastic-plastic) and strength behaviors of fixed-ended hat and zed-section columns strongly affected by strong local-distortional interaction (nearly coincident buckling loads) – moreover, these results are also compared with similar ones reported earlier for fixed-ended lipped channel columns (Silvestre *et al.* 2009, 2012).

### 2.1 Buckling Behavior

Trial-and-error buckling analyses, carried out for lipped channel columns, led to the identification of a common column geometry ensuring practically identical local and distortional critical buckling loads for the three cross-section shapes:  $b_w=150\text{ mm}$  (web height),  $b_f=140\text{ mm}$  (flange width),  $b_s=10\text{ mm}$  (lip width),  $t=1.3\text{ mm}$  (wall thickness) and  $L=90\text{ cm}$  (length). Figs. 2(a)-(b) show (i) curves providing the variation of  $P_{cr}$  (critical buckling load) with the column length  $L$  (in logarithmic scale) for fixed-ended lipped channel (C curve), hat-section (H curve) and zed-section (Z curve) columns and (ii) hat and zed-section  $L_{LD}=90\text{ cm}$  column “mixed” (L-D) critical buckling mode shapes, yielded by ABAQUS analyses. The observation of these buckling results prompts the following remarks:

- (i) The  $P_{cr}$  vs.  $L$  curves exhibit three distinct zones, corresponding to buckling in (i<sub>1</sub>) local (1-5 half-waves), (i<sub>2</sub>) distortional (1-11 half-waves for H and C columns and 1-16 half-waves for Z columns) and (i<sub>3</sub>) flexural-torsional buckling (single half-wave) – moreover, note the fuzzy transition between the length intervals associated with L and D critical buckling, which typically occurs in fixed-ended columns (unlike in their pin-ended counterparts, most of which exhibit a very clear transition).
- (ii) The C, H and Z column critical buckling curves only differ in the length corresponding to the transition between distortional and global (flexural-torsional) buckling – it occurs for  $L_{D/FT}=950\text{ cm}$  (H columns),  $L_{D/FT}=1000\text{ cm}$  (C columns) and  $L_{D/FT}=1350\text{ cm}$  (Z columns). Taking the C columns as

---

<sup>2</sup> The column are discretized into fine 4-node isoparametric shell element meshes (length-to-width ratio roughly equal to 1), the fixed-ended conditions are modeled by attaching rigid plates to the column end sections and the steel material behavior is described by a linear-elastic/perfectly-plastic stress-strain curve (both residual stresses and corner effects are disregarded) – a detailed account of all modeling issues can be found in Dinis & Camotim (2006, 2012) and Dinis *et al.* (2007).

<sup>3</sup> It is worth noting that recent investigations by Silvestre *et al.* (2012) and Young *et al.* (2012) have shown that considerable column ultimate strength erosion may also occur when the local critical buckling is well below its distortional counterpart, provided that the yield stress is high enough to allow for the development of significant local-distortional. This specific issue already began to be investigated by the first two authors (Dinis *et al.* 2009b) and constitutes a topic of current research – additional results will most likely be reported in the near future.

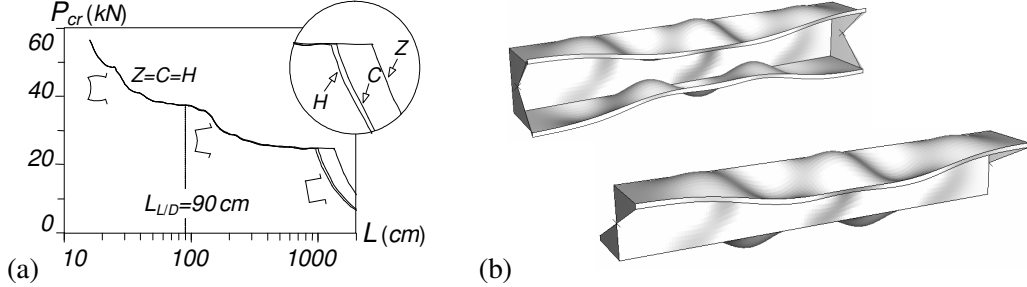


Figure 2: (a) C, H and Z column critical buckling curves and (b) H and Z column “mixed” L-D critical buckling modes (for  $L_{LD}$ )

- reference, the flexural-torsional buckling loads (ii<sub>1</sub>) considerably increase in the Z columns, due to the much higher (almost double) major-axis inertia, (ii<sub>2</sub>) slightly decrease in the H columns, due to the lower (by about 10%) warping constant, which outshines the marginally higher major-axis inertia.
- (iii) For columns shorter than the H column transition length ( $L < 950\text{cm}$ ), all the local and distortional critical buckling loads virtually identical, even if the H column distortional values are a tiny bit (less than 0.5%) above their C and Z column counterparts.
  - (iv) The  $L_{LD}=90\text{cm}$  C, H and Z columns buckle for  $P_{cr}=37.3\text{kN}$  ( $f_{cr}=63.8\text{MPa}$ ) in a mode combining arbitrarily (iv<sub>1</sub>) a single distortional half-wave and (iv<sub>2</sub>) 5 local half-waves – the last two column critical buckling modes shapes are depicted in Fig. 2(b). Obviously, the post-buckling behaviors and ultimate strengths of these three columns will be strongly affected by local-distortional interaction.

## 2.2 Initial Geometrical Imperfections

The initial geometrical imperfection shape always plays a crucial role in mode interaction investigations, since its choice may alter considerably the post-buckling behavior and strength of the structural system under consideration. Therefore, it is necessary to study and compare the post-buckling behaviors of otherwise identical members containing various critical-mode initial imperfection shapes, combining differently the two competing L and D buckling modes and sharing the same overall amplitude (Dinis *et al.* 2007). In this study, the H and Z column initial imperfection shapes are similar to those considered earlier for the lipped channel columns (Dinis *et al.* 2009a) and consist of linear combinations of (i) five half-wave local and (ii) a single half-wave distortional buckling modes, both normalized to exhibit

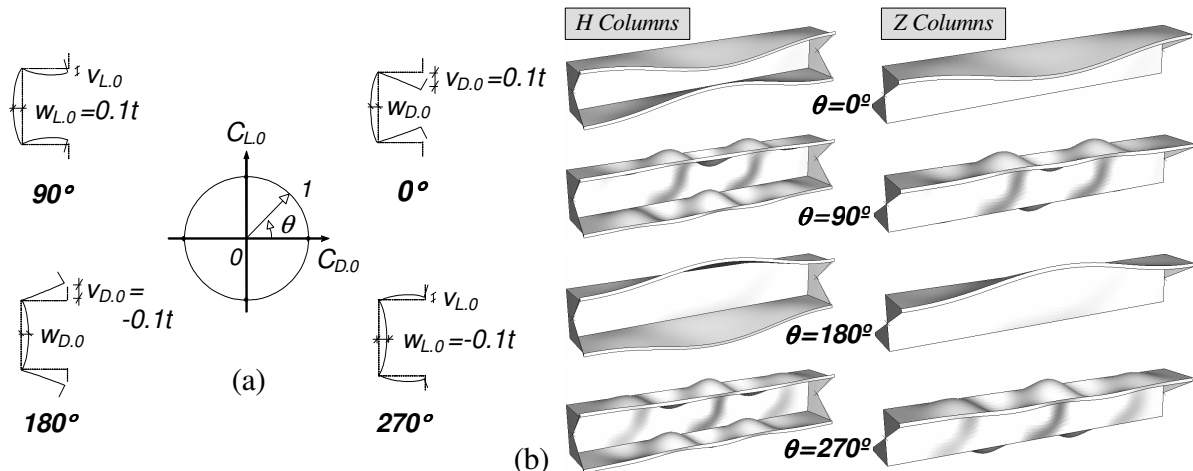


Figure 3: (a) Initial imperfection representation in the  $C_{D,0}$ - $C_{L,0}$  plane (H columns) and (b) initial imperfection shapes for  $\theta=0^\circ, 90^\circ, 180^\circ$  and  $270^\circ$  (H and Z columns)

amplitudes equal to 10% of the wall thickness  $t$  ( $0.1t=0.13\text{ mm}$ ). The combination coefficients,  $C_{L,0}$  and  $C_{D,0}$ , satisfy the condition  $(C_{L,0})^2+(C_{D,0})^2=1$ , and each initial imperfection shape is defined by an angle  $\theta$ , such that  $C_{L,0}=\sin\theta$  and  $C_{D,0}=\cos\theta$ , as illustrated in Fig. 3(a) for the H columns. Fig. 3(b) displays the pure local ( $\theta=90^\circ$  or  $270^\circ$  – outward/inward mid-span web bending) and distortional ( $\theta=0^\circ$  or  $180^\circ$  – inward/outward mid-span top flange-lip transverse motions) imperfections for the H and Z columns.

### 2.3 Elastic Post-Buckling Behavior

This section addresses the elastic post-buckling behavior of the fixed-ended hat and zed-section columns previously identified (in 2.1). In order to assess how the initial geometrical imperfection shape influences the post-buckling behavior under strong L-D interaction in the column post-buckling, numerical results concerning (i) H columns with imperfection shapes defined by  $\theta=0^\circ, 45^\circ, 90^\circ, 135^\circ, 180^\circ, 225^\circ, 270^\circ, 315^\circ$ , and (ii) Z columns with imperfection shapes defined by  $\theta=0^\circ, 45^\circ, 90^\circ$ <sup>4</sup> are presented and discussed – for clarification purposes, Z columns with  $\theta=5^\circ, 10^\circ, 25^\circ, 30^\circ, 180^\circ$  initial imperfections have also been analyzed and the corresponding post-buckling results are presented.

Figs. 4(a)-(b) show the upper portions ( $P/P_{cr}>0.6$ ) of the elastic equilibrium paths (i)  $P/P_{cr}$  vs.  $v/t$ , where  $v$  is the mid-span top flange-lip corner vertical displacement<sup>5</sup>, and (ii)  $P/P_{cr}$  vs.  $w/t$ , where  $w$  is the mid-span mid-web flexural displacement, for the H (Figs. 4(a<sub>1</sub>)-(b<sub>1</sub>)) and Z (Figs. 4(a<sub>2</sub>)-(b<sub>2</sub>)) columns analyzed. As for Figs. 4(c<sub>1</sub>)-(c<sub>2</sub>), they show the deformed configurations of six columns at advanced post-buckling stages, namely (i)  $\theta=0^\circ, 90^\circ, 225^\circ$  H and (ii)  $\theta=0^\circ, 25^\circ, 90^\circ$  Z columns. The observation of all these post-buckling results leads to the following conclusions:

- (i) The column deformed configurations associated with all equilibrium paths shown in Fig. 4(a)-(b) combine (i<sub>1</sub>) predominant single half-wave distortional deformations, which are responsible for the whole  $v$  values and also part of the  $w$  values, with (i<sub>2</sub>) less relevant five half-wave local deformations, responsible for the remaining part of the  $w$  values – Fig. 4(c) displays six column deformed configurations exhibiting these combined features. Moreover, note that the emergence (i<sub>1</sub>) of local deformations in the  $\theta=0^\circ$  and  $\theta=180^\circ$  columns ( $C_{L,0}=0$ ), and (i<sub>2</sub>) of distortional deformations in the  $\theta=90^\circ$  and  $\theta=270^\circ$  columns ( $C_{D,0}=0$ ) provides clear evidence of the occurrence of L-D interaction.
- (ii) It is clear that the  $P/P_{cr}$  vs.  $w/t$  equilibrium paths are much more “irregular” than their  $P/P_{cr}$  vs.  $v/t$  counterparts, which is due to the fact that they “mix” distortional and local deformations with quite different half-wave numbers. Thus, H and Z column post-buckling behaviors will be assessed next exclusively through the analysis of the  $P/P_{cr}$  vs.  $w/t$  equilibrium paths – the (difficult) interpretation of the  $P/P_{cr}$  vs.  $w/t$  equilibrium paths will be specifically addressed a bit further ahead in the paper – see Figs. 5(a)-(b) and the corresponding comments.
- (iii) The equilibrium paths concerning the (iii<sub>1</sub>)  $\theta=0^\circ-270^\circ-315^\circ$  and (iii<sub>2</sub>)  $\theta=45^\circ-90^\circ-135^\circ-180^\circ$  H columns merge into common curves. Since the  $\theta=225^\circ$  column equilibrium path remains a single curve, it may be said that the 8 hat-section column equilibrium paths “evolve” towards one of 3 curves, associated with inward (one of them) or outward (the other two) mid-span flange-lip motions.
- (iv) The existence of more than two “merging curves”, described in the previous item, was also reported in the fixed-ended H columns affected by L-D interaction analyzed by Dinis *et al.* (2011). However, this does not occur in fixed-ended lipped channel columns, as all equilibrium paths merge into just 2 curves, involving inward or outward mid-span flange-lip motions (Dinis *et al.* 2009a).

<sup>4</sup> Since the Z column local and distortional post-buckling behaviors are both symmetric, there is no need to present post-buckling results concerning the  $\theta>90^\circ$  columns (*i.e.*, only the first  $C_{D,0}-C_{L,0}$  plane quadrant needs to be considered).

<sup>5</sup> The distinction between the top and bottom flange-lip corner is relevant only for the Z columns – indeed, both flange-lip corners move identically in the H columns.

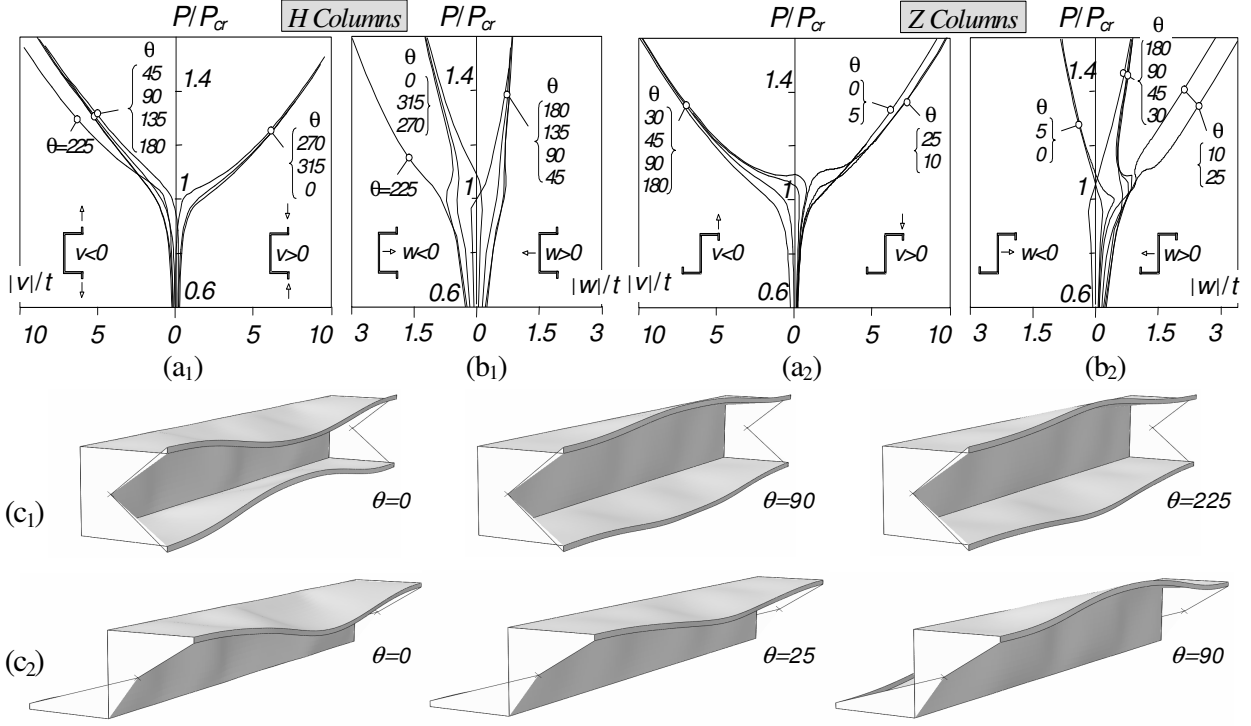


Figure 4: (a)  $P/P_{cr}$  vs.  $v/t$  and (b)  $P/P_{cr}$  vs.  $w/t$  equilibrium paths, and (c) three deformed configurations at advanced post-buckling stages for the (1) H and (2) Z columns

- (v) For H columns, the pure distortional initial imperfections with *inward* mid-span flange-lip motions ( $\theta=0^\circ$ ) are the *most detrimental*, in the sense that the associated equilibrium path lies below all the others (*i.e.*, exhibit lower strengths) – the same occurred in the H columns recently analyzed by Dinis *et al.* (2011). Note that pure distortional initial imperfections with *outward* mid-span flange-lip motions are the most detrimental in fixed-ended lipped channel (C) columns (Dinis *et al.* 2009a).
- (vi) Finally, the Z columns also exhibit three “merging curves” (two of them very close), concerning columns exhibiting initial imperfections defined by  $0^\circ \leq \theta \leq 25^\circ$  (*inward* mid-span top flange-lip motions) and  $30^\circ \leq \theta \leq 180^\circ$  (*outward* mid-span top flange-lip motions), respectively – note that the  $\theta=180^\circ$  column has exactly the same post-buckling behavior and strength of the  $\theta=0^\circ$  one, as they only differ in the role reversal exhibited by the top and bottom flange-lip assemblies. Moreover, the pure distortional ( $\theta=0^\circ$  or  $\theta=180^\circ$ ) initial imperfections are again the most detrimental ones in the fixed-ended Z columns (like in the H and C columns, as seen just before).

In order to explain why the H and Z (and C) columns exhibit more than two “merging curves”, Figs. 5(a)-(b) provide, for six different columns ( $\theta=0^\circ, 90^\circ, 225^\circ$  H and  $\theta=0^\circ, 25^\circ, 90^\circ$  Z columns), the web deformed configurations ( $w/t$ ) at three equilibrium states, corresponding to increasing  $P/P_{cr}$  values. It is worth noting that (i) each web deformed configuration concerns a column whose behavior is described by one of the “merging curves”, (ii) positive  $w$  correspond to *outward* web bending (to the top flange left), and (iii) the horizontal coordinate is normalized with respect to the column length –  $x_3/L$ . The analysis of these web deformed configuration evolutions prompts the following remarks:

- (i) For  $P/P_{cr} < 0.8$ , the  $\theta=0^\circ, 90^\circ$  column web deformed configurations are akin to the initial imperfection shape, *i.e.*, exhibit 1 ( $\theta=0^\circ$ ) or 5 ( $\theta=90^\circ$ ) half-waves, respectively. For higher  $P/P_{cr}$  values, these configurations change and become a combination of the two above components, thus providing clear evidence of the occurrence of L-D interaction.

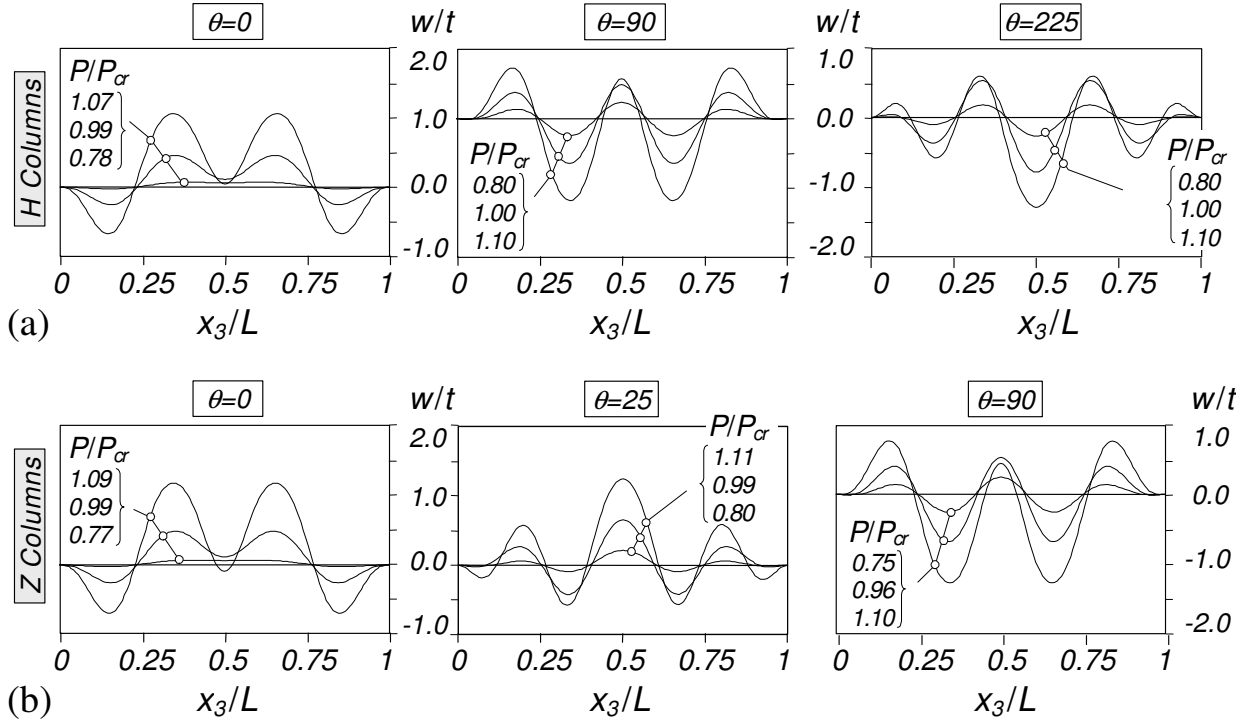


Figure 5 Web deformed configuration evolutions (three load values) for the (a) H and (b) Z columns

- (ii) In the  $\theta=0^\circ$  columns, the web configurations change mentioned in the previous item leads to a decrease (and subsequent reversal) of the mid-span  $w$  value. In the  $\theta=90^\circ$  columns, on the other hand, this change causes a mid-span  $w$  increase. This reflects the fact that the mid-span web flexural displacement stemming from the local deformations either opposes ( $\theta=0^\circ$ ) or reinforces ( $\theta=90^\circ$ ) its distortional counterpart.
- (iii) The  $\theta=225^\circ$  H and  $\theta=25^\circ$  Z columns exhibit an additional behavioral feature in the advanced post-buckling stages ( $P/P_{cr} \geq 1.1$ ): the development of higher “localized” deformations in the mid-span region (central half-wave), due to a stronger mutual interaction/reinforcement of the distortional and local deformations – in the  $\theta=0^\circ$  and  $\theta=90^\circ$  columns such deformation “localization” occurs in the two half-waves adjacent to the central one and involve deformed configuration distortional components with opposite signs. Although the mechanical explanation for the singular behaviors of these two columns is not yet completely clear for the authors, it is worth noting that the above initial imperfection shapes are associated with sudden “sign transitions” of the deformed configuration distortional component (see Figs. 4(a<sub>1</sub>) and 4(b<sub>1</sub>)) – somehow these “transitions” seem to favour the occurrence of the web deformation “localization” in the central half-wave.

The common post-buckling equilibrium paths plotted in Figs. 4(a)-(b), (e.g., those concerning H columns with initial imperfections defined by  $0^\circ < \theta \leq 180^\circ$ ) correspond to column deformed configurations that may be deemed to define, approximately, “coupled buckling mode shapes”. In order to quantify the amount of “coupling” and, at the same time, provide a better visualization of this concept, a “mode coupling ratio”  $C_L/C_D$  is defined – it relates the amplitudes of the column deformed configuration local and distortional components. These amplitudes are obtained on the basis of the mid-span (i) web mid-point flexural displacement  $w$  and (ii) top flange-lip corner displacement  $v$ , by adopting the following assumptions and methodology:

- (i) The column deformed configuration can be completely expressed as a linear combination of the local and distortional critical buckling mode shapes, normalized with respect to  $w_{L,0}=v_{D,0}=1\text{ mm}$ .
- (ii) The  $v$  and  $w$  values associated with a given deformed configuration stem exclusively from its distortional and local components.
- (iii) The value of  $w$  comprises two parts, due to the local ( $w_L$ ) and distortional ( $w_D$ ) components. The second one can be readily determined by using the fact that the distortional buckling mode shape is characterized by the ratio  $w \approx 0.216 v$  (H columns) or  $w \approx 0.242 v$  (Z columns).
- (iv) In view of the above assumptions, the values of  $C_D$  and  $C_L$  are given by the expressions

$$C_D = v/v_{D,0} \quad (1)$$

$$C_L = (w - 0.216 v)/w_{L,0} \quad (\text{H columns}) \quad C_L = (w - 0.242 v)/w_{L,0} \quad (\text{Z columns}) \quad . \quad (2)$$

Figs. 6(a)-(b) provide the evolution, along the post-buckling equilibrium paths, of the “mode coupling ratio”  $C_L/C_D$ , for columns containing initial imperfection defined by (i)  $0^\circ \leq \theta \leq 180^\circ + 270^\circ \leq \theta \leq 360^\circ$  (H columns –  $\theta=15^\circ$  intervals) and (ii)  $0^\circ \leq \theta \leq 5^\circ + 30^\circ \leq \theta \leq 180^\circ$  (Z columns –  $\theta=15^\circ$  intervals) – the selected  $\theta$  values correspond to columns whose deformed configuration evolution may rightly be deemed expressed as a linear combination of the competing L and D critical buckling modes. The curves in Figs. 6(a)-(b) provide valuable information about the H and Z column local-distortional interactive behavior:

- (i) All curves (i<sub>1</sub>) start at different points on a unit radius circle centered at the origin and (i<sub>2</sub>) have initial slopes given by the corresponding initial imperfection shapes – see the details in Figs. 6(a)-(b).
- (ii) The various  $C_L/C_D$  curves converge to practically straight lines with different slopes, namely (ii<sub>1</sub>)  $\Delta C_L \approx -0.36 \Delta C_D$  ( $C_D > 0$  – inward flange-lip motions) and  $\Delta C_L \approx -0.28 \Delta C_D$  ( $C_D < 0$  – outward flange-lip motions), for H columns, and (ii<sub>2</sub>)  $\Delta C_L \approx \pm 0.33 \Delta C_D$ , for Z columns. It seems realistic to argue that such straight lines define the (predominantly distortional) column “coupled buckling modes”.

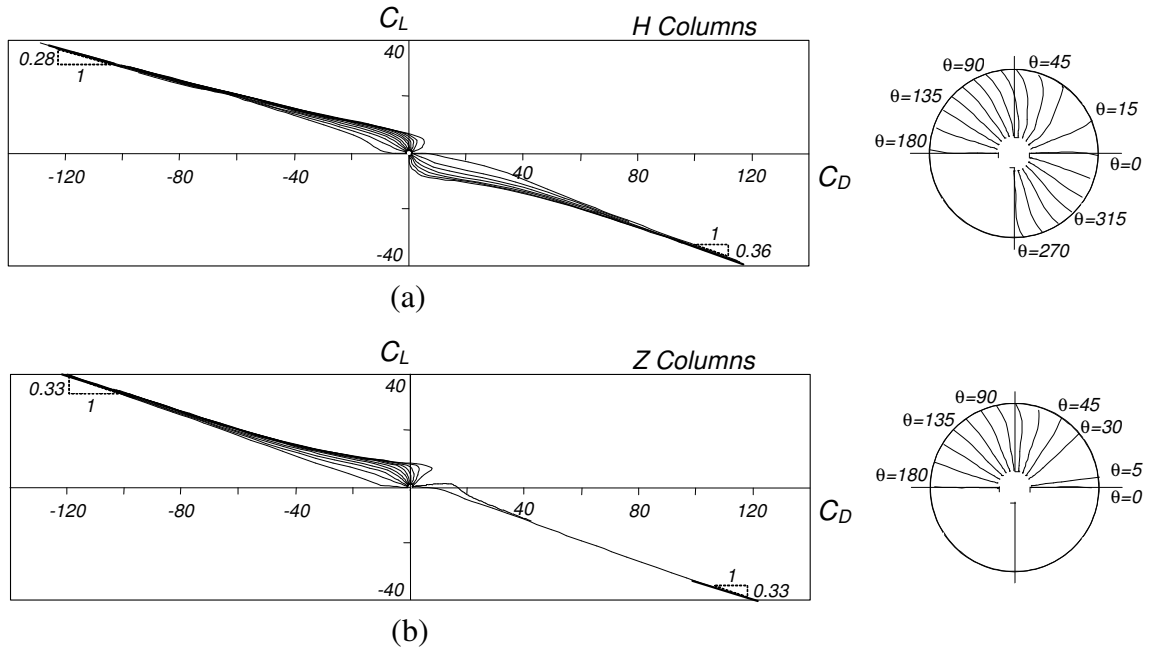


Figure 6: Evolution of the mode coupling ratio  $C_L/C_D$  along the equilibrium paths of the (a) H and (b) Z columns

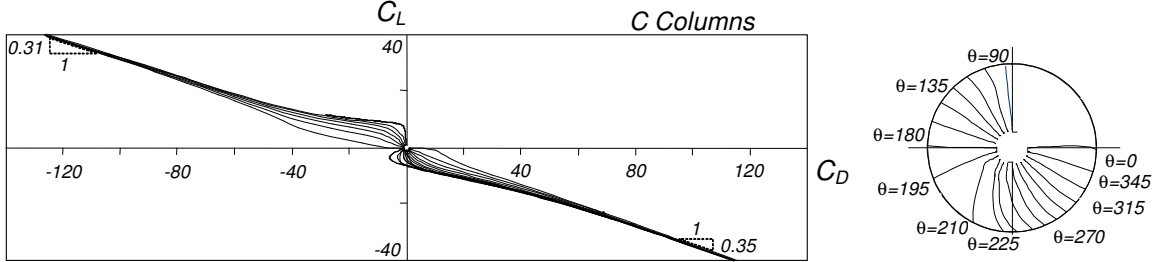


Figure 7: Evolution of the mode coupling ratio  $C_L/C_D$  along the equilibrium paths of the lipped channel columns

- (iii) The different slopes of the lines associated with inward or outward H column flange-lip motions are due to the non-negligible asymmetry characterizing their distortional post-buckling behavior (e.g., Dinis *et al.* 2011). Obviously, the Z column lines share exactly the same slope, thus reflecting the symmetric distortional post-buckling behavior of these columns (one flange-lip assembly moves inward and the other outward).
- (iv) For both column geometries, the two “coupled mode” straight lines correspond to  $C_D$  and  $C_L$  values with opposite signs. This indicates that the corresponding column deformed configurations combine local and distortional mid-web flexural displacements *opposing* each other at the mid-span region (see Figs. 5(a)-(b)) – since the distortional and local buckling mode exhibits a single and five half-waves, respectively, this also means that these flexural displacements *reinforce* each other in other regions of the column.
- (v) The characteristics described in the previous items (specially for the H columns) are similar to those unveiled for lipped channel (C) columns with the same geometry (also strongly affected by local-distortional interaction), as shown Fig. 7. Indeed, the various  $C_L/C_D$  curves converged to two straight lines with slopes  $\Delta C_L \approx -0.35 \Delta C_D$  ( $C_D > 0$  – inward flange-lip motions) and  $\Delta C_L \approx -0.31 \Delta C_D$  ( $C_D < 0$  – outward flange-lip motions). These values are perfectly in line with those obtained in this work for the H and Z columns.
- (vi) The C and H column mode coupling ratio diagram exhibit “missing portions” (columns with initial imperfections not leading to the “coupled buckling mode” deformed configurations) corresponding to  $0^\circ < \theta < 90^\circ$  and  $180^\circ < \theta < 270^\circ$ , respectively. Since the stiffer distortional post-buckling behavior corresponds to (vi<sub>1</sub>) inward top flange-lip motions in the C columns ( $\theta=0^\circ$ ) and (vi<sub>2</sub>) outward flange-lip motions in the H columns ( $\theta=180^\circ$ ), the two  $\theta$  ranges are indeed associated with the same initial imperfection characteristics: local flexural displacements *reinforcing* those stemming from the *stiffer* distortional component in the mid-span region.

#### 2.4 Elastic-Plastic Post-Buckling Behavior

Next, the elastic/perfectly-plastic post-buckling behavior of fixed ended hat and zed-section columns undergoing L-D interaction is investigated – due to space limitations, only a few of the most relevant results obtained are presented and discussed. They concern H and Z columns (i) containing initial  $\theta=0^\circ$  initial imperfections shapes (the most detrimental for both column types, as found from the elastic post-buckling analyses) and (ii) exhibiting *three* yield-to-critical stress ratios, namely  $f_y/f_{cr} \approx 1.2, 2.4, 3.9$ , corresponding to yield stresses equal to  $f_y = 75, 150, 250 \text{ MPa}$  – recall that  $f_{cr} = f_L = f_D \approx 63.5 \text{ MPa}$ . For comparative purposes, some elastic results presented earlier are shown again – they may be viewed as associated with an infinite yield stress (*i.e.*,  $f_y = f_y/f_{cr} = \infty$ ).

Fig. 8(a) shows the upper portions ( $P/P_{cr} > 0.6$ ) of four equilibrium paths  $P/P_{cr}$  vs.  $v/t$  corresponding to the H columns exhibiting the four different yield-to-critical stress ratios. As for Fig. 8(b), it concerns the

column with  $f_y/f_{cr} \approx 2.4$  and displays three plastic strain diagrams, corresponding to the equilibrium state locations indicated on its equilibrium path, in Fig. 8(a), and including the collapse mechanism. Finally, Figs. 9(a)-(b) show similar elastic-plastic results for Z columns also containing pure distortional initial imperfections – in order to clarify the plastic strain evolution in these columns, two views are shown for each equilibrium state. The observation of all these results makes it possible to conclude that:

- (i) The nature and characteristics of the H and Z column elastic-plastic post-buckling behavior and collapse mechanism are clearly dependent on the values of the  $f_y/f_{cr}$  ratio.
- (ii) In the columns with a  $f_y/f_{cr}$  close to 1.0 (e.g.,  $f_y/f_{cr} \approx 1.2$ ), first yielding occurs when the column normal stress distribution is still “fairly uniform” and, therefore, precipitates a rather “abrupt” collapse – yielding occurs in a significant portion of the “most deformed (critical) cross-section”, whose location depends on the initial imperfection shape (mid-span, for the  $\theta=0^\circ$  columns considered here).
- (iii) In the columns with a higher  $f_y/f_{cr}$  value (e.g.,  $f_y/f_{cr}=2.4, 3.9$ ), first yielding occurs when the column normal stress distribution is already “heavily non-uniform” and, therefore, does not lead to an immediate collapse – instead, collapse occurs after a mild “snap-through” phenomenon, followed by a subsequent strength increase up to a limit point, as illustrated in Figs. 8(a) and 9(a).
- (iv) The yielding pattern and the failure mechanism of the  $\theta=0^\circ$  H and Z columns are quite different: while the former exhibit symmetry (both flange-lip assemblies are involved), the latter are clearly asymmetric (mostly the bottom flange-lip assembly, which moves *outward*, is involved). Indeed, for the H columns, (iv<sub>1</sub>) yielding begins at both lip free end zones, in the vicinity of the column mid-span (diagram I in Fig. 8(b)), and (iv<sub>2</sub>) collapse occurs after the full yielding of the web-flange corners at

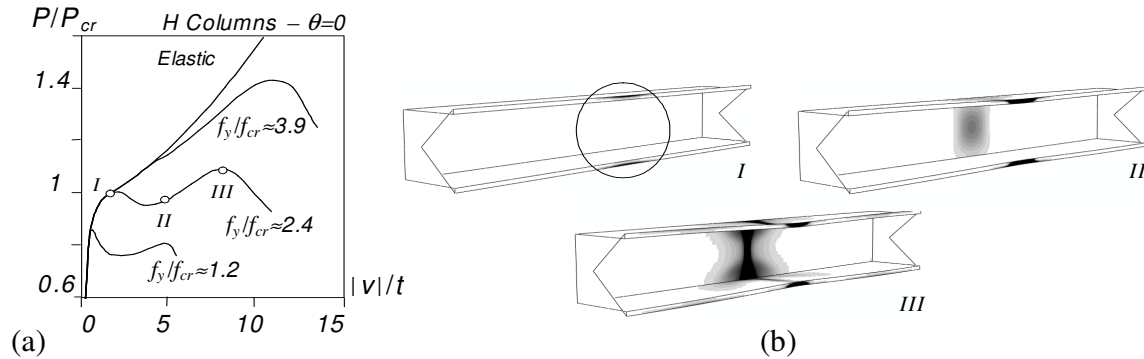


Figure 8: H column (a) elastic-plastic  $P/P_{cr}$  vs.  $v/t$  equilibrium paths ( $\theta=0^\circ + f_y/f_{cr} \approx 1.2, 2.4, 3.9, \infty$ ) and (b) deformed configurations and plastic strain evolutions at three equilibrium states ( $\theta=0^\circ + f_y/f_{cr} \approx 2.4$ )

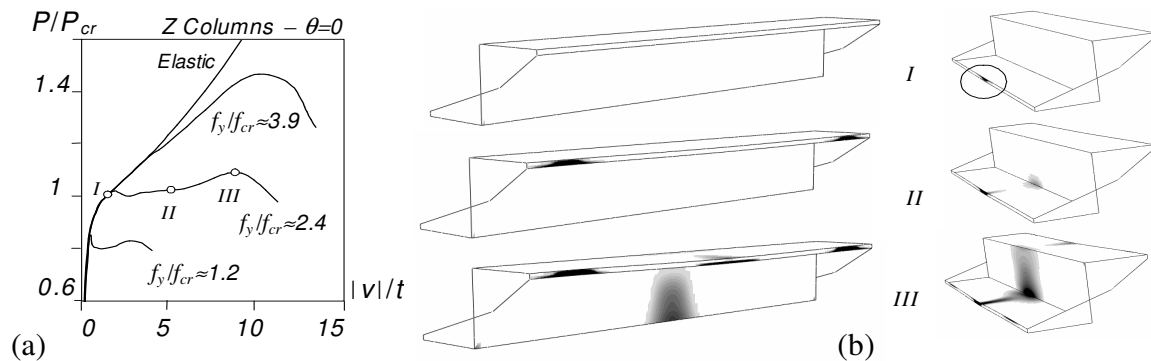


Figure 9: Z column (a) elastic-plastic  $P/P_{cr}$  vs.  $v/t$  equilibrium paths ( $\theta=0^\circ + f_y/f_{cr} \approx 1.2, 2.4, 3.9, \infty$ ) and (b) deformed configurations and plastic strain evolutions at three equilibrium states ( $\theta=0^\circ + f_y/f_{cr} \approx 2.4$ )

the column central region – the failure mechanism corresponds to the formation of a “distortional plastic hinge” at mid-span (diagram *III* in Fig. 8(b)). For the Z columns, however, the onset of yielding and failure mechanism involve mostly the column mid-span bottom lip, flange and web-flange corner, as depicted in diagrams *I* and *III* of Fig. 9(b) – note, however, that yielding also progresses along the column top lip regions near the column supports prior to collapse (this does not happen in the H columns, where yielding is restricted to the mid-span region).

### 3. Parametric Study: Scope and Numerical Results

The first step of this parametric study consisted of identifying several column geometries (cross-section dimensions and lengths) associated with practically identical local and distortional critical buckling loads/stresses. Taking advantage of the fact, illustrated in Fig. 2(a), that C, H and Z and columns sharing the same geometry have identical local and distortional (not global) buckling stresses, this identification is a straightforward matter: the 14 geometries identified in the context of lipped channel columns (Silvestre *et al.* 2012) as having  $f_{cr,L} \approx f_{cr,D}$  are now used in the present parametric study, dealing with hat and zed-section columns. These geometries are used as *reference cases* and slight variations in the flange ( $b_f$ ), web ( $b_w$ ) or lip/stiffener ( $b_s$ ) width generate additional column geometries that exhibit distinct, but fairly close,  $f_{cr,L}$  and  $f_{cr,D}$  values ( $0.90 \leq f_{cr,L}/f_{cr,D} \leq 1.10$ ), just as was done for the lipped channel columns – a total of 42 column geometries are included in the parametric study. In order to cover a wide distortional (and local) slenderness  $\lambda = (f_y/f_{cr,D})^{0.5}$  range, 5 different yield stresses are considered for each of the 42 columns ( $f_y = 150, 250, 350, 550, 750 \text{ MPa}$ ), which implies that 210 H and Z column pairs were analyzed. The analyses are performed by means of ABAQUS elastic-perfectly plastic shell finite element analyses (SFEA) that neglect both the corner effects and residual stresses (the latter were shown to have little effect on the ultimate strength of cold-formed steel columns – *e.g.*, Ellobody & Young 2005). Moreover, regardless of the critical stress ratio  $f_{cr,L}/f_{cr,D}$ , all columns contain critical-mode distortion initial imperfections with (i) *inward* top flange-lip motions of the central half-wave (buckling modes with odd distortion half-wave numbers)<sup>6</sup> and (ii) small amplitude (maximum top flange-lip corner vertical displacement equal to 10% of the wall thickness  $t$ ). All the column cross-section dimensions ( $b_w, b_f, b_s, t$ ), lengths ( $L$ ), buckling stresses ( $f_{cr,L}, f_{cr,D}$ ), yield stresses ( $f_y$ ) and SFEA ultimate stresses ( $f_u$ ) are given in Annexes A (H columns) and B (Z columns) – in order to enable a direct and easy comparison with the lipped channel column results obtained previously (Silvestre *et al.* 2012), they are included in Annex C.

### 4. Direct Strength Method (DSM) Design – Assessment of the Ultimate Strength Estimates

The currently available DSM design curves for cold formed steel columns consist of “Winter-type” expressions that (i) were calibrated against fairly large numbers of experimental and/or numerical results and (ii) provide safe and accurate ultimate strength estimates associated with local, distortional or global (flexural or flexural-torsional) failures on the sole basis of elastic buckling and yield stresses – the DSM expressions prescribing the column nominal strengths against local ( $f_{NL}$ ), distortional ( $f_{ND}$ ) and ( $f_{NE}$ ) collapses can be found in Schafer’s state-of-the-art report (2008). Moreover, in order to capture also local-global interactive failures, the current DSM replaces  $f_y$  by  $f_{NE}$  in the  $f_{NL}$  expressions, thus providing  $f_{NLE}$  estimates. On the other hand, two distinct strategies were also proposed by Schafer (2002) to estimate the ultimate strength of columns experiencing L-D interaction: replacing  $f_y$  either (i) by  $f_{ND}$  in the  $f_{NL}$  equations (NLD approach –  $f_{NLD}$ ) or (ii) by  $f_{NL}$  in the  $f_{ND}$  equations (NDL approach –  $f_{NDL}$ ) – soon after, Yang & Hancock (2004) adopted the NLD approach to investigate the L-D interaction in lipped channel

---

<sup>6</sup> Recall that (i) the distinction between top and bottom flange-lip assemblies only is needed in the Z columns and (ii) in columns buckling in modes with even distortional half-wave numbers, the flange-lip motion sense (inward or outward) is not relevant.

columns with “v-shape” web and flange intermediate stiffeners and found that the estimates obtained were always safe and reasonably accurate (differences within the 10-20% range). Later, Silvestre *et al.* (2009) assessed the performance of these two approaches in the context of plain lipped channel columns, and concluded that they yielded basically similar results, even if the “quality” of the  $f_{NDL}$  estimates was marginally higher – this explains the use of the NDL approach in this work, which means that the column ultimate strength estimate is given by

$$f_{NDL} = f_{NL} \quad \text{if} \quad \lambda_{DL} \leq 0.561 \quad , \quad (3)$$

$$f_{NDL} = f_{NL} \left( \frac{f_D}{f_{NL}} \right)^{0.6} \left[ 1 - 0.25 \left( \frac{f_D}{f_{NL}} \right)^{0.6} \right] \quad \text{if} \quad \lambda_{DL} > 0.561$$

where  $\lambda_{DL} = (f_{NL}/f_D)^{0.5}$  is the “distortional-local slenderness”. Quite recently, Silvestre *et al.* (2012) proposed a novel DSM approach to predict more accurately the ultimate strength of fixed lipped channel columns experiencing L-D interaction ( $f^*_{NDL}$ ). For columns with low-to-moderate D slenderness ( $\lambda_D < 1.5$ ), the  $f^*_{NDL}$  values coincide with the  $f_{ND}$  ones, *i.e.*, the current DSM distortional strength curve is retained. For the more slender columns ( $\lambda_D \geq 1.5$ ), the novel approach (i) defines a modified local strength  $f^*_{NL}$ , which depends on the critical half-wave length ratio  $L_{crD}/L_{crL}$ , obtained from the simply supported column “signature curve”, and (ii) provides column ultimate strength estimates through the replacement of  $f_{NL}$  by  $f^*_{NL}$  in the NDL equations – the  $f^*_{NL}$  values are given by

$$\begin{aligned} f^*_{NL} &= f_y \quad \text{if} \quad \frac{L_{crD}}{L_{crL}} \leq 4 \\ f^*_{NL} &= f_y + \left( 1 - 0.25 \frac{L_{crD}}{L_{crL}} \right) (f_y - f_{NL}) \quad \text{if} \quad 4 < \frac{L_{crD}}{L_{crL}} < 8 \\ f^*_{NL} &= f_{NL} \quad \text{if} \quad \frac{L_{crD}}{L_{crL}} \geq 8 \end{aligned} . \quad (4)$$

Note that these equations lead to  $f_{ND}$  and  $f_{NLD}$  when  $L_{crD}/L_{crL} \leq 4$  and  $L_{crD}/L_{crL} \geq 8$ , respectively. The tables included in Annexes A-C present the various DSM ultimate strength estimates ( $f_{NL}, f_{ND}, f_{NE}, f_{NLE}, f_{NDL}, f^*_{NDL}$ ) and relevant quantities involved in their calculation, namely the distortional slenderness  $\lambda_D$  and the *simply supported* column distortion and local critical half-wave lengths  $L_{crD}$  and  $L_{crL}$  (determined by means of GBT buckling analyses), for the H (Annex A), Z (Annex B) and C (Annex C) columns – in the latter case, the vast majority of the values presented have already been reported by Silvestre *et al.* 2012.

Figs. 10(a)-(c) show the variation of  $f_{ND}/f_U$ ,  $f_{NLD}/f_U$  and  $f^*_{NDL}/f_U$  with  $\lambda_D$  for the H (Figs. 10(a<sub>1</sub>)-(c<sub>1</sub>)) and Z (Figs. 10(a<sub>2</sub>)-(c<sub>2</sub>)) columns – the corresponding averages and standard deviations are given in Table 1. The analysis of these results prompts the following comments<sup>7</sup>:

- (i) For 12 H and 9 Z columns, the lowest DSM ultimate strength estimate is  $f_{NLE}$ , thus indicating a local-global interactive collapse. Since the visual inspection of the corresponding SFEA collapse modes showed (i<sub>1</sub>) clear evidence of distortional (mostly) and local deformations, and (i<sub>2</sub>) no trace of global deformations, such columns are treated here as failing in local-distortional interactive modes.

---

<sup>7</sup> The  $f_{NL}$  and  $f_{NLE}$  values presented in the tables included in Annexes A-C are not displayed in Fig. 10. This is because they clearly overestimate and underestimate, respectively, the column ultimate strengths and, thus, do not deserve further attention.

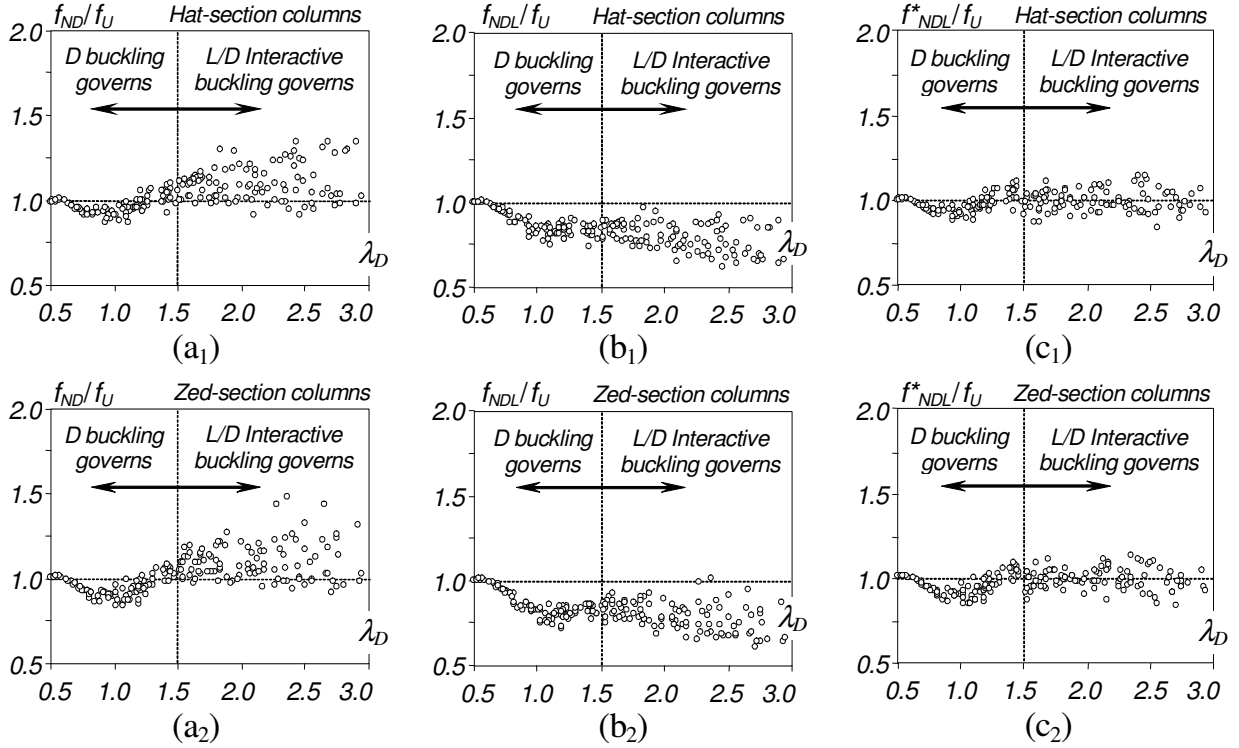


Figure 10: Variation of (a)  $f_{ND}/f_U$ , (b)  $f_{NDL}/f_U$  and (c)  $f^*_{NDL}/f_U$  with the distortional slenderness  $\lambda_D$  for the (1) H and (2) Z columns

Table 1: Averages and standard deviations of the H and Z column ultimate strength estimates

	H Columns			Z Columns		
	$\frac{f_{ND}}{f_U}$	$\frac{f_{NDL}}{f_U}$	$\frac{f^*_{NDL}}{f_U}$	$\frac{f_{ND}}{f_U}$	$\frac{f_{NDL}}{f_U}$	$\frac{f^*_{NDL}}{f_U}$
Average	1.04	0.81	0.97	1.03	0.81	0.96
Standard Deviation	0.10	0.10	0.07	0.11	0.11	0.07

- (ii) For both the H and Z columns, all the  $f_{ND}/f_U$ ,  $f_{NDL}/f_U$  and  $f^*_{NDL}/f_U$  ultimate strength estimates ratios have quite similar variations with  $\lambda_D$  – this statement can be clearly observed in Figs. 10(a<sub>1</sub>)-(c<sub>2</sub>).
- (iii) The  $f_{ND}$  values provide reasonably accurate column ultimate strength estimates. Indeed, the  $f_{ND}/f_U$  values exhibit the following characteristics: (iii<sub>1</sub>) 1.04 average, 0.10 standard deviation, 88 safe and accurate values ( $0.90 < f_{ND}/f_U \leq 1.0$ ), 67 a bit unsafe values ( $1.00 < f_{ND}/f_U \leq 1.10$ ), 6 too safe values ( $f_{ND}/f_U \leq 0.90$ ) and 49 too unsafe values ( $f_{ND}/f_U \geq 1.10$ ), for the H columns, and (iii<sub>2</sub>) 1.03 average, 0.11 standard deviation, 84 safe and accurate values, 62 a bit unsafe values, 19 too safe values and 45 too unsafe values, for the Z columns. However, Figs. 10(a<sub>1</sub>)-(a<sub>2</sub>) provide evidence that the  $f_{ND}$  values (iii<sub>1</sub>) exhibit errors that clearly grow with  $\lambda_D$ , (iii<sub>2</sub>) are accurate and mostly safe for  $\lambda_D < 1.5$  (less relevant L-D interaction effects), and (iii<sub>3</sub>) inaccurate and mostly unsafe for  $\lambda_D \geq 1.5$ . This means that the  $f_{ND}$  values cannot predict adequately the erosion suffered by the column distortional ultimate strength due to the L-D mode interaction effects.
- (iv) The  $f_{NDL}$  estimates are quite conservative and exhibit little scatter. Indeed, the  $f_{NDL}/f_U$  values are characterized by: (iv<sub>1</sub>) 0.81 average, 0.10 standard deviation, 28 safe and accurate values, 177 too safe values and only 5 too unsafe values, for the H columns, and (iv<sub>2</sub>) 0.81 average, 0.11 standard

- deviation, 24 safe and accurate values, 177 too safe values and only 9 too unsafe values, for the Z columns. Figs. 10(b<sub>1</sub>)-(b<sub>2</sub>) show that a large fraction of the “too safe estimates” occurs for  $\lambda_D \geq 1.5$ .
- (v) The  $f_{NDL}^*$  estimates are fairly accurate and also exhibit little scatter. Indeed, the  $f_{NDL}^*/f_U$  values exhibit the following characteristics: (v<sub>1</sub>) 0.97 average, 0.07 standard deviation, 118 safe and accurate values, 61 a bit unsafe values, 25 too safe values, and just 6 too unsafe values (maximum  $f_{NDL}^*/f_U$  is 1.15), for the H columns, and (v<sub>2</sub>) 0.96 average, 0.07 standard deviation, 108 safe and accurate values, 64 a bit unsafe values, 38 too safe values and just 4 too unsafe values (maximum  $f_{NDL}^*/f_U$  is 1.13), for the Z columns. The “quality” of the  $f_{NDL}^*$  can be assessed by looking at Figs. 10(a)-(c), clearly showing how close the  $f_{NDL}^*/f_U$  values are from the “unit horizontal line” – recall that they are coincident with the  $f_{NDL}/f_U$  values for the low-to-moderate distortional slenderness range ( $\lambda_D < 1.5$ ).
  - (vi) The  $f_{NDL}/f_U$ ,  $f_{NDL}/f_U$  and  $f_{NDL}^*/f_U$  values are quite similar to those reported by Silvestre *et al.* (2012) for the fixed-ended C columns, shown in Figs. 11(a)-(c) – their averages and standard deviations were found to be equal to (vi<sub>1</sub>) 1.04; 0.11, (vi<sub>2</sub>) 0.82; 0.11 and (vi<sub>3</sub>) 0.97; 0.07, respectively<sup>8</sup>. This confirms that, as it would be logical to expect, the ultimate strengths of the H, Z and C column trios sharing the same geometry are practically identical also in the presence of strong L-D interaction.

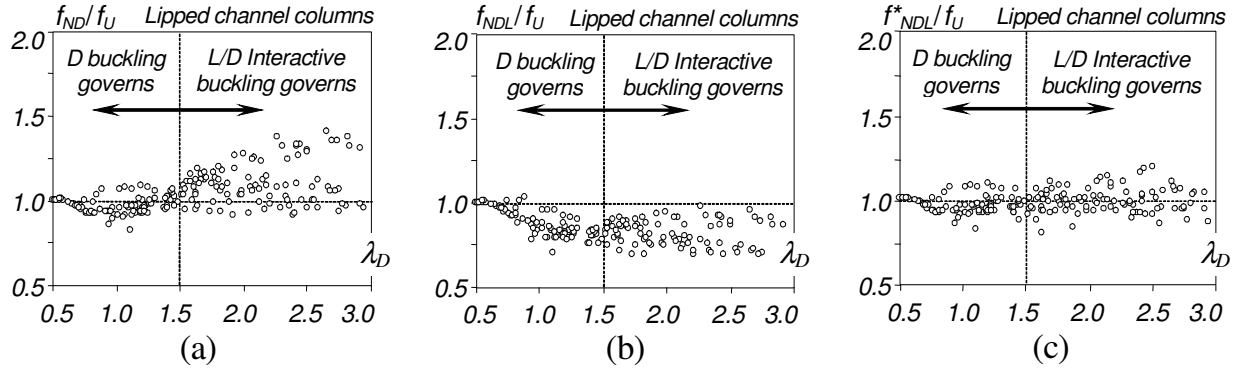


Figure 11: Variation of (a)  $f_{NDL}/f_U$ , (b)  $f_{NDL}/f_U$  and (c)  $f_{NDL}^*/f_U$  with the distortional slenderness  $\lambda_D$  for the C columns

Finally, Figs. 12(a)-(b) show (i) the variation of  $f_U/f_y$  (white dots) and  $f_{NDL}^*/f_y$  (grey dots) with  $\lambda_D$ , and (ii) the DSM “Winter-type curves” providing the  $f_{NL}/f_y$ ,  $f_{ND}/f_y$  and  $f_{NDL}/f_y$  (assuming that  $f_L=f_D$ ) values, for the H (Figs. 12(a<sub>1</sub>)-(b<sub>1</sub>)) and Z (Figs. 12(a<sub>1</sub>)-(b<sub>1</sub>)) columns. These plots make it possible to conclude that:

- (i) Both the H and Z columns exhibit (i<sub>1</sub>)  $f_U/f_y$  values that remain quite “aligned” with a “Winter-type curve”, and (i<sub>2</sub>) a reasonably small “vertical dispersion” that grows with  $\lambda_D$ . Moreover, they lie (i<sub>1</sub>) above the  $f_{NDL}/f_y$  and  $f_{NDL}^*/f_y$  curves (much closer to the former), for  $\lambda_D < 1.5$ , and (i<sub>2</sub>) between the D and DL curves, for  $\lambda_D \geq 1.5$ .
- (ii) Since the  $f_U/f_y$  and  $f_{NDL}^*/f_y$  value distributions (“clouds”) depicted in Figs. 12 are virtually identical to those obtained by Silvestre *et al.* (2012) for the C columns and shown in Figs. 13(a)-(b), it is not surprising to find out that the novel DSM approach proposed by these authors also provides accurate and safe ultimate strength estimates for the H and Z columns dealt with in this work – note that each column trio (same cross-section dimensions and length) shares the same  $f_L, f_D, L_{crL}, L_{crD}$  values.
- (iii) The  $f_{NDL}^*/f_y$  values are on the current distortional strength curve for (iii<sub>1</sub>)  $\lambda_D < 1.5$  (stocky columns) and (iii<sub>2</sub>)  $\lambda_D \geq 1.5$  (slender columns) with low  $L_{crD}/L_{crL}$  ratios (no relevant L-D interaction). But they lie well below that curve for  $\lambda_D \geq 1.5$  and moderate-to-high  $L_{crD}/L_{crL}$  values (relevant L-D interaction).

<sup>8</sup> It is worth noting that the H and Z column geometries considered in this work are only a subset (although a fairly one – 210 vs. 276) of the C columns analyzed and reported by Silvestre *et al.* (2012).

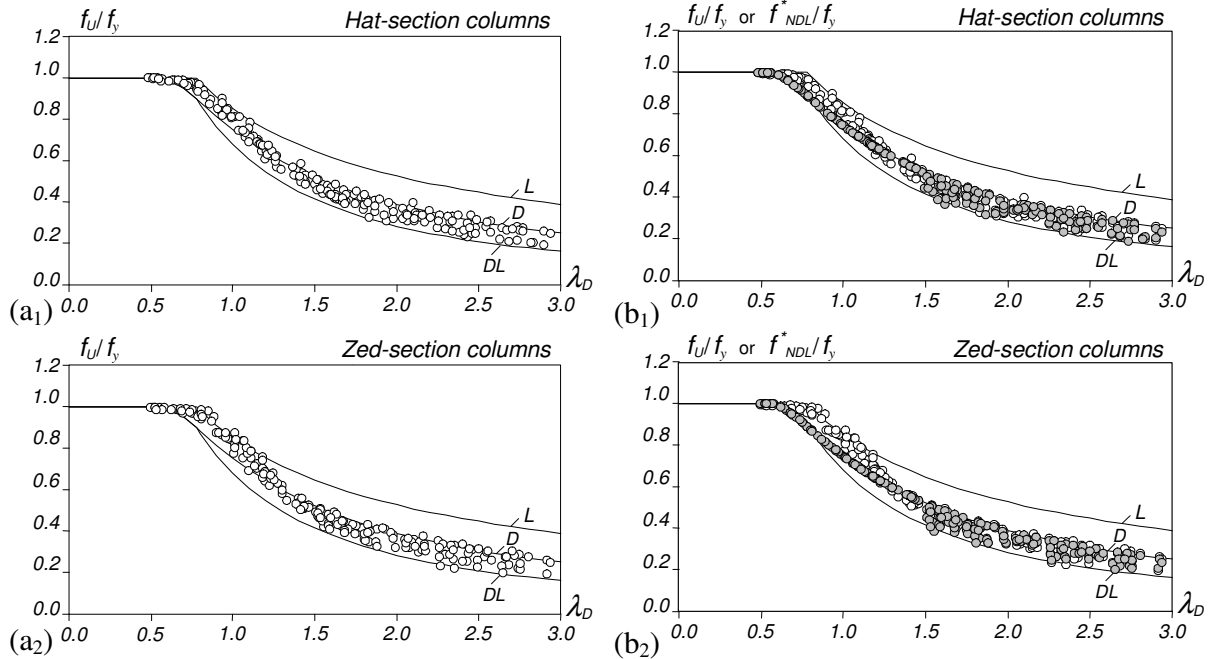


Figure 12: Variation of the (a)  $f_U/f_y$  and (b)  $f_U/f_y + f^*_{NDL}/f_y$  values with  $\lambda_D$  for the (1) H and (2) Z columns

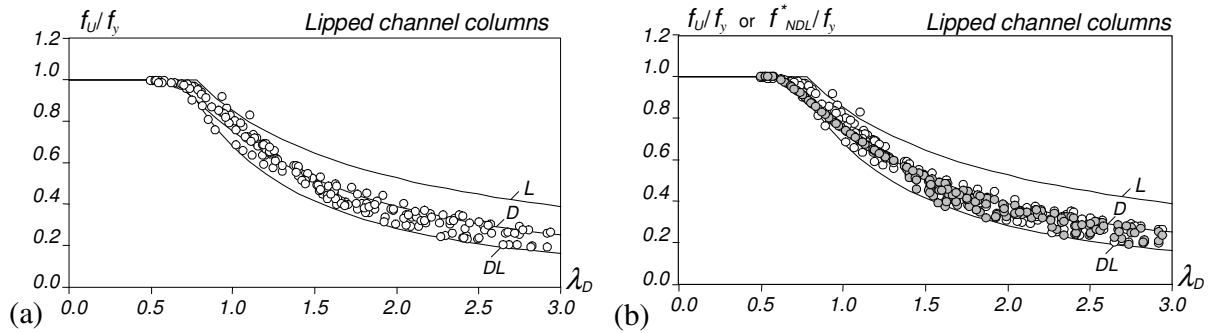


Figure 13: Variation of the (a)  $f_U/f_y$  and (b)  $f_U/f_y + f^*_{NDL}/f_y$  values with  $\lambda_D$  for the C columns (from Silvestre *et al.* 2012)

## 5. Concluding Remarks

This paper reported the latest results of an ongoing investigation on the post-buckling behavior, strength and design of cold-formed steel columns, aimed at extending recent findings obtained for lipped channel columns to other cross-section shapes. After comparing the elastic and elastic-plastic post-buckling and strength behaviors of hat-section (H), zed-section (Z) and lipped channel (C) fixed-ended columns sharing cross-section dimensions and lengths that lead to virtually identical local and distortional buckling loads (high susceptibility to local-distortional interaction and identical buckling behaviors), the paper presented and discussed the results of an extensive ABAQUS shell finite element parametric study, aimed at determining the “exact” ultimate loads of 210 pairs of initially imperfect H and Z columns with various geometries, all associated with strong local-distortional interaction (identical to those exhibited by C columns analyzed in previous investigations). The ultimate strength data gathered from the above parametric study were then used to assess the performance of a recently proposed (in the context of C columns) novel DSM-based approach aimed at estimating efficiently (safely and accurately) the ultimate strength of cold-formed steel fixed-ended columns undergoing strong local-distortional interaction, namely when applied to similar H and Z columns under the same circumstances.

The H and Z column buckling and post-buckling results made it possible (i) to confirm the anticipated similarities with the C column behavior and also (ii) to explain the few discrepancies unveiled during this investigation. Moreover, it was shown that the novel DSM-based design approach proposed by Silvestre *et al.* (2012), which (i) is specifically intended to estimate column ultimate strengths associated with local-distortional interactive failures (nearly coincident local and distortional critical buckling loads), (ii) was recently developed/validated in the context of fixed-ended lipped channel columns and (iii) is based on values of elastic critical (local and distortional) buckling stresses and critical half-wave length ratios  $L_{crD}/L_{crL}$ , can also be successfully applied to predict hat and zed-section column ultimate strengths.

Finally, one last word to mention that further research is currently under way, in order to investigate whether this DSM-based design approach can be extended to columns exhibiting additional cross-section shapes, namely rack-sections – part of the outcome of this research effort, which was initiated a few years ago (Silvestre *et al.* 2008), will be reported in the very near future (Dinis *et al.* 2012).

## References

- AISI – American Iron and Steel Institute (2007). *North American Specification for the Design of Cold-Formed Steel Structural Members* (NAS), Washington DC.
- AS/NZS – Standards of Australia and Standards of New Zealand (2005). *Cold-Formed Steel Structures*, Sydney-Wellington.
- Camotim D, Dinis PB, Silvestre N (2008). “Local/distortional mode interaction in lipped channel steel columns: post-buckling behaviour, strength and DSM design”, *Proceedings of Fifth International Conference on Thin-Walled Structures - Recent Innovations and Developments* (ICTWS 2008 – Brisbane, 18-20/6), 281-288 (vol. 1).
- Dinis PB, Camotim D (2006). “On the use of shell finite element analysis to assess the local buckling and post-buckling behaviour of cold-formed steel thin-walled members”, ”, *Book of Abstracts of III European Conference on Computational Mechanics: Solids, Structures and Coupled Problems in Engineering* (III ECCM – Lisboa, 5-9/6), C.A.M. Soares *et al.* (eds.), Springer, 689. (full paper in CD-ROM Proceedings)
- Dinis PB, Camotim D (2010). “Local/distortional mode interaction in cold-formed steel lipped channel beams”, *Thin-Walled Structures*, **48**(10-11), 771-785.
- Dinis PB, Camotim D (2012). “On the shell finite element buckling and post-buckling analysis of cold-formed steel members”, *submitted for publication*.
- Dinis PB, Camotim D, Silvestre N (2007). “FEM-based analysis of the local-plate/distortional mode interaction in cold-formed steel lipped channel columns”, *Computers & Structures*, **85**(19-20), 1461-1474.
- Dinis PB, Young B, Camotim D (2009a). “On the effect of local/distortional mode interaction on the post-buckling behaviour and ultimate strength of fixed-ended lipped channel columns”, *Proceedings of IJSSD Symposium on Progress in Structural Stability and Dynamics* (Hong Kong, 16-18/12), 191-198.
- Dinis PB, Silvestre N, Camotim D (2009b). “On the relevance of local/distortional interaction in the post-buckling behaviour and strength of cold-formed steel lipped channel columns”, *Proceedings of Twelfth International Conference on Civil, Structural and Environmental Engineering Computing* (CC 2009 – Funchal, 1-4/9), B. Topping, L.C. Neves, R.C. Barros (eds.), Civil-Comp Press, paper 22. (full paper in CD-ROM Proceedings)
- Dinis PB, Camotim D, Fena R (2011). “Local/distortional mode interaction in hat-section columns: post-buckling behaviour, strength and DSM design”, *Proceedings of Sixth European Conference on Steel and Composite Structures* (EUROSTEEL 2011 – Budapest, 31/8-2/9), 69-74 (vol. A).
- Dinis PB, Camotim D, Fena R. (2012). “On the DSM design of cold-formed steel columns against local-distortional interactive failure”, *Proceedings of 10<sup>th</sup> International Conference on Advances in Steel, Concrete, Composite and Hybrid Structures* (ASCCS 2012 – Singapore, 2-4/7), in press.
- Ellobody E, Young B (2005). “Behavior of cold-formed steel plain angle columns”, *Journal of Structural Engineering* (ASCE), **131**(3), 469-478, 2005.
- Hancock GJ, Kwon YB, Bernard ES (1994). “Strength design curves for thin-walled members”, *Journal of Constructional Steel Research*, **31**(3), 169-186.
- Kwon YB, Kim BS, Hancock GJ (2009). “Compression tests of high strength cold-formed steel channels with buckling interaction”, *Journal of Constructional Steel Research*, **65**(2), 278-289.

- Schafer BW (2002). "Local, distortional and Euler buckling in thin-walled columns", *Journal of Structural Engineering* (ASCE), **128**(3), 289-299.
- Schafer BW (2008). "Review: the Direct Strength Method of cold-formed steel member design", *Journal of Constructional Steel Research*, **64**(7-8), 766-778.
- Schafer BW, Peköz T (1998). "Direct strength prediction of cold-formed steel members using numerical elastic buckling solutions", *Thin-Walled Structures - Research and Development* (ICTWS'98 – Singapore, 2-4/12), N. Shanmugam, J.Y.R. Liew, V. Thevendran (eds.), Elsevier, 137-144.
- Simulia Inc. (2008). *Abaqus Standard* (vrs. 6.7-5).
- Silvestre N, Dinis PB, Camotim D (2008). "DSM design of simply supported rack-section columns against local-distortional interactive buckling", *Proceedings of 5<sup>th</sup> International Conference on Coupled Instabilities in Metal Structures* (CIMS 2008 – Sydney, 23-24/6), K. Rasmussen, T. Wilkinson (eds.), 417-424.
- Silvestre N, Camotim D, Dinis PB, (2009). "Direct strength prediction of lipped channel columns experiencing local-plate/distortional interaction", *Advanced Steel Construction*, **5**(1), 45-67.
- Silvestre N, Camotim D, Dinis PB (2012). "Post-buckling behaviour and direct strength design of lipped channel columns experiencing local/distortional interaction", *Journal of Constructional Steel Research*, in press.
- Yang D, Hancock GJ (2004). "Compression tests of high strength steel columns with interaction between local and distortional buckling", *Journal of Structural Engineering* (ASCE), **130**(12), 1954-1963.
- Yap DCY, Hancock GJ (2011). Experimental study of high strength cold-formed stiffened web steel sections, *Journal of Structural Engineering* (ASCE), **137**(2), 162-172.
- Young B, Camotim D, Silvestre N (2009). "Ultimate strength and design of lipped channel columns experiencing local/distortional mode interaction – Part I: experimental investigation", *Proceedings of Sixth International Conference on Advances in Steel Structures* (ICASS'09 – Hong Kong, 16-18/12), 460-469 (vol. I).
- Young B, Silvestre N, Camotim D (2012). "Cold-formed steel lipped channel columns influenced by local-distortional interaction: strength and DSM design", *submitted for publication*.

## ANNEX A

Table A1: H columns: SFEA ultimate strengths and corresponding DSM estimates (dimensions in *mm*, stresses in *MPa*) – I

		GBT			SFEA				DSM											
		L	L <sub>cr.D</sub>	L <sub>cr.L</sub>	f <sub>E</sub>	f <sub>D</sub>	f <sub>L</sub>	f <sub>y</sub>	f <sub>U</sub>	λ <sub>D</sub>	f <sub>NL</sub>	f <sub>ND</sub>	f <sub>NE</sub>	f <sub>NLE</sub>	f <sub>NDL</sub>	f <sup>*</sup> <sub>NDL</sub>	f <sub>NL</sub> / <sub>f<sub>U</sub></sub>	f <sub>ND</sub> / <sub>f<sub>U</sub></sub>	f <sub>NDL</sub> / <sub>f<sub>U</sub></sub>	f <sup>*<sub>NDL</sub>/<sub>f<sub>U</sub></sub></sup>
<i>b<sub>w</sub>=100, b<sub>s</sub>=100, t=1.9mm</i>	<i>b<sub>s</sub>=17.5</i>	<i>1760</i>	<i>745 100 471,7</i>	<i>262,2 262,2 350 245</i>	150	145	0,76	150	136	131	131	136	136	1,03	0,94	0,94	0,94			
					250	213	0,98	216	191	200	186	174	191	1,01	0,90	0,82	0,90			
					550	275	1,16	270	232	257	220	200	232	1,10	0,95	0,82	0,95			
					750	303	1,45	363	296	338	264	237	296	1,32	1,08	0,86	1,08			
					150	147	1,69	444	346	386	288	265	278	1,47	1,14	0,87	0,92			
	<i>b<sub>s</sub>=20</i>	<i>1760</i>	<i>815 100 457,7</i>	<i>284,6 262,9 350 274</i>	150	147	0,73	150	139	131	131	139	139	1,02	0,95	0,95	0,95			
					250	225	0,94	216	197	199	185	180	197	0,96	0,88	0,80	0,88			
					550	298	1,11	270	241	254	218	207	241	0,99	0,88	0,76	0,88			
					750	316	1,39	364	308	333	261	246	308	1,22	1,03	0,83	1,03			
					150	147	1,62	444	361	378	284	275	275	1,41	1,14	0,87	0,87			
<i>b<sub>w</sub>=100, b<sub>s</sub>=10, t=1.0mm</i>	<i>b<sub>s</sub>=16</i>	<i>1760</i>	<i>700 100 481,1</i>	<i>243,4 261,5 350 228</i>	150	142	0,79	150	134	132	132	134	134	1,06	0,94	0,94	0,94			
					250	203	1,01	216	185	201	186	170	185	1,06	0,91	0,84	0,91			
					550	269	1,20	270	225	258	220	194	225	1,18	0,99	0,85	0,99			
					750	302	1,50	363	286	341	265	229	245	1,35	1,06	0,85	0,91			
					150	147	1,76	444	333	391	290	255	278	1,47	1,10	0,85	0,92			
	<i>b<sub>w</sub>=95</i>	<i>2500</i>	<i>595 85 223,0</i>	<i>103,9 103,9 350 114</i>	150	91	1,20	113	96	113	94	82	96	1,24	1,06	0,90	1,06			
					250	111	1,55	157	126	156	116	99	106	1,42	1,13	0,89	0,96			
					550	148	1,84	195	149	181	128	111	122	1,71	1,30	0,97	1,07			
					750	157	2,30	261	184	196	134	128	145	1,76	1,24	0,87	0,98			
					150	91	2,69	317	212	196	134	142	163	2,02	1,35	0,90	1,04			
<i>b<sub>w</sub>=80, b<sub>s</sub>=10, t=1.0mm</i>	<i>b<sub>w</sub>=88</i>	<i>2500</i>	<i>585 85 193,2</i>	<i>108,2 114,7 350 127</i>	150	97	1,18	117	98	108	94	85	98	1,20	1,01	0,87	1,01			
					250	115	1,52	163	128	145	114	103	111	1,42	1,12	0,89	0,96			
					550	151	1,80	203	152	164	124	115	127	1,59	1,19	0,91	1,00			
					750	165	2,25	270	188	169	126	134	151	1,79	1,24	0,88	1,00			
					150	94	2,63	329	216	169	126	147	170	1,99	1,31	0,89	1,03			
	<i>b<sub>w</sub>=105</i>	<i>2500</i>	<i>605 90 267,4</i>	<i>93,0 89,0 350 108</i>	150	94	1,27	107	91	119	92	76	91	1,14	0,97	0,81	0,97			
					250	103	1,64	149	119	169	116	91	101	1,45	1,16	0,88	0,98			
					550	128	1,94	185	140	202	130	102	116	1,71	1,30	0,95	1,07			
					750	152	2,43	246	173	233	142	118	139	1,92	1,35	0,92	1,09			
					150	94	2,84	299	199	235	143	130	157	1,97	1,31	0,86	1,03			
<i>b<sub>w</sub>=80, b<sub>s</sub>=10, t=1.5mm</i>	<i>b<sub>w</sub>=114</i>	<i>1150</i>	<i>500 95 1451,2</i>	<i>172,0 172,0 350 190</i>	150	126	0,93	133	119	144	129	110	119	1,06	0,94	0,87	0,94			
					250	162	1,21	187	160	233	179	136	160	1,16	0,99	0,84	0,99			
					550	234	1,43	234	191	316	219	154	191	1,23	1,01	0,81	1,01			
					750	277	1,79	313	240	469	283	180	223	1,34	1,02	0,77	0,95			
					150	124	2,09	382	278	604	332	200	257	1,38	1,00	0,72	0,93			
	<i>b<sub>w</sub>=120</i>	<i>1150</i>	<i>505 100 1583,1</i>	<i>167,5 157,1 350 186</i>	150	124	0,95	129	117	144	126	107	117	1,04	0,95	0,86	0,95			
					250	158	1,22	182	158	234	174	132	158	1,15	1,00	0,83	1,00			
					550	230	1,45	226	189	319	213	150	189	1,22	1,01	0,80	1,01			
					750	262	1,81	303	236	476	276	175	222	1,32	1,03	0,76	0,97			
					150	128	2,12	369	274	615	325	194	256	1,41	1,05	0,74	0,98			
<i>b<sub>w</sub>=106</i>	<i>1150</i>	<i>495 90 1277,4</i>	<i>180,8 194,4 350 196</i>	<i>180,8 194,4 350 196</i>	150	128	0,91	139	121	143	134	115	121	1,08	0,94	0,90	0,94			
					250	168	1,18	195	163	230	185	142	163	1,16	0,97	0,85	0,97			
					550	241	1,39	244	196	312	226	161	196	1,24	1,00	0,82	1,00			
					750	279	1,74	327	246	459	291	189	227	1,36	1,02	0,78	0,94			
					150	128	2,04	399	285	587	341	210	260	1,43	1,02	0,75	0,93			

Table A2: H columns: SFEA ultimate strengths and corresponding DSM estimates (dimensions in  $mm$ , stresses in  $MPa$ ) – II

		GBT			SFEA			DSM													
		L	$L_{cr,D}$	$L_{cr,L}$	$f_E$	$f_D$	$f_L$	$f_y$	$f_U$	$\lambda_D$	$f_{NL}$	$f_{ND}$	$f_{NE}$	$f_{NLE}$	$f_{NDL}$	$f^{*}_{NDL}$	$\frac{f_{NL}}{f_U}$	$\frac{f_{ND}}{f_U}$	$\frac{f_{NDL}}{f_U}$	$\frac{f^{*}_{NDL}}{f_U}$	
$b_w=100, b_s=10, t=2,4mm$	$b_l=55$	620	310	80	3342,1	150	150	0,50	150	150	147	147	150	150	1,00	1,00	1,00	1,00	1,00	1,00	1,00
						250	248	0,65	250	243	242	242	243	243	1,01	0,98	0,98	0,98	1,01	0,98	0,98
						590,8	589,0	0,77	350	315	335	335	315	315	1,03	0,92	0,92	0,92	1,03	0,92	0,92
						550	464	0,96	478	424	513	456	389	424	1,03	0,91	0,84	0,91	1,03	0,91	0,84
						750	539	1,13	588	509	683	553	442	509	1,09	0,94	0,82	0,94	1,09	0,94	0,82
$b_w=100, b_s=10, t=2,4mm$	$b_l=50$	620	290	80	3137,1	150	150	0,49	150	150	147	147	150	150	1,00	1,00	1,00	1,00	1,00	1,00	1,00
						250	248	0,63	250	246	242	242	246	246	1,01	0,99	0,99	0,99	1,01	0,99	0,99
						625,4	598,1	0,75	350	320	334	334	320	320	1,02	0,93	0,93	0,93	1,02	0,93	0,93
						550	483	0,94	481	434	511	457	398	434	0,99	0,90	0,82	0,90	0,99	0,90	0,82
						750	560	1,10	591	522	679	553	453	522	1,06	0,93	0,81	0,93	1,06	0,93	0,81
$b_w=100, b_s=10, t=1,9mm$	$b_l=60$	620	325	85	3513,5	150	149	0,52	150	150	147	147	150	150	1,01	1,01	1,01	1,01	1,01	1,01	1,01
						250	246	0,67	250	241	243	243	241	241	1,02	0,98	0,98	0,98	1,02	0,98	0,98
						558,9	581,2	0,79	350	310	336	336	310	310	1,05	0,93	0,93	0,93	1,05	0,93	0,93
						550	443	0,99	476	415	515	455	380	415	1,07	0,94	0,86	0,94	1,07	0,94	0,86
						750	517	1,16	586	497	686	552	431	497	1,13	0,96	0,83	0,96	1,13	0,96	0,83
$b_w=100, b_s=10, t=1,9mm$	$b_l=110$	1030	590	150	4401,6	150	104	1,15	116	100	148	115	86	100	1,12	0,96	0,83	0,96	1,12	0,96	0,83
						250	133	1,49	162	131	244	160	104	131	1,22	0,99	0,78	0,99	1,22	0,99	0,78
						113,1	113,1	1,76	201	155	339	197	117	155	1,28	0,98	0,74	0,98	1,28	0,98	0,74
						550	198	2,21	269	192	522	260	136	192	1,36	0,97	0,69	0,97	1,36	0,97	0,69
						750	233	2,58	327	222	698	313	150	222	1,40	0,95	0,64	0,95	1,40	0,95	0,64
$b_w=100, b_s=10, t=1,9mm$	$b_l=130$	1030	655	160	4735,7	150	94	1,22	115	95	148	114	81	95	1,22	1,01	0,86	1,01	1,22	1,01	0,86
						250	120	1,58	160	123	245	158	98	123	1,33	1,03	0,82	1,02	1,33	1,03	0,82
						100,0	108,8	1,87	199	146	339	195	110	145	1,39	1,02	0,77	1,01	1,39	1,02	0,77
						550	181	2,35	265	180	524	257	127	179	1,46	0,99	0,70	0,99	1,46	0,99	0,70
						750	213	2,74	322	207	702	309	140	206	1,51	0,97	0,66	0,97	1,51	0,97	0,66
$b_w=180, b_s=20, t=4,0mm$	$b_l=90$	1030	515	145	3883,1	150	114	1,10	117	104	148	116	90	104	1,03	0,91	0,79	0,91	1,03	0,91	0,79
						250	147	1,42	164	137	243	161	109	137	1,11	0,93	0,74	0,93	1,11	0,93	0,74
						124,3	116,4	1,68	204	163	337	199	123	163	1,27	1,02	0,77	1,02	1,27	1,02	0,77
						550	219	2,10	272	202	518	262	143	202	1,24	0,92	0,65	0,92	1,24	0,92	0,65
						750	254	2,46	331	233	692	314	158	233	1,30	0,92	0,62	0,92	1,30	0,92	0,62
$b_w=180, b_s=20, t=4,0mm$	$b_l=100$	2000	620	145	1044,6	150	150	0,54	150	150	141	141	150	150	1,00	1,00	1,00	1,00	1,00	1,00	1,00
						250	247	0,70	250	237	226	226	237	237	1,01	0,96	0,96	0,96	1,01	0,96	0,96
						510,9	501,5	0,83	334	301	304	303	292	301	1,02	0,92	0,89	0,92	1,02	0,92	0,89
						550	412	1,04	453	400	441	391	356	400	1,10	0,97	0,86	0,97	1,10	0,97	0,86
						750	472	1,21	557	477	555	456	403	477	1,18	1,01	0,85	1,01	1,18	1,01	0,85
$b_w=180, b_s=20, t=4,0mm$	$b_l=90$	2000	580	145	978	150	150	0,52	150	150	141	141	150	150	1,00	1,00	1,00	1,00	1,00	1,00	1,00
						250	248	0,67	250	241	225	225	241	241	1,01	0,97	0,97	0,97	1,01	0,97	0,97
						554,0	508,1	0,79	336	309	301	301	300	309	0,99	0,91	0,89	0,91	0,99	0,91	0,89
						550	448	1,00	455	414	435	389	368	414	1,02	0,92	0,82	0,92	1,02	0,92	0,82
						750	512	1,16	559	495	544	452	418	495	1,09	0,97	0,82	0,97	1,09	0,97	0,82
$b_w=180, b_s=20, t=4,0mm$	$b_l=110$	2000	660	150	1099,3	150	149	0,57	150	150	142	142	150	150	1,01	1,01	1,01	1,01	1,01	1,01	1,01
						250	244	0,73	250	231	227	227	231	231	1,02	0,95	0,95	0,95	1,02	0,95	0,95
						463,8	494,4	0,87	333	292	306	304	282	292	1,06	0,93	0,90	0,93	1,06	0,93	0,90
						550	392	1,09	451	384	446	392	342	384	1,15	0,98	0,87	0,98	1,15	0,98	0,87
						750	429	1,27	554	457	564	459	386	457	1,29	1,06	0,90	1,06	1,29	1,06	0,90

Table A3: H columns: SFEA ultimate strengths and corresponding DSM estimates (dimensions in  $mm$ , stresses in  $MPa$ ) – III

		GBT			SFEA			DSM														
		L	$L_{cr,D}$	$L_{cr,L}$	$f_E$	$f_D$	$f_L$	$f_y$	$f_U$	$\lambda_D$	$f_{NL}$	$f_{ND}$	$f_{NE}$	$f_{NLE}$	$f_{NDL}$	$f^*_{NDL}$	$\frac{f_{NL}}{f_U}$	$\frac{f_{ND}}{f_U}$	$\frac{f_{NDL}}{f_U}$	$\frac{f^*_{NDL}}{f_U}$		
$b_w=110, b_i=85, t=2.4mm$	$b_s=15$	940	545	95	1947,2	471,5	458,8	350	305	150	148	0,56	150	150	145	145	150	150	1,01	1,01	1,01	1,01
										250	240	0,73	250	232	237	237	232	232	1,04	0,97	0,97	0,97
										550	393	0,86	325	293	325	309	279	293	1,07	0,96	0,92	0,96
										750	447	1,08	440	387	489	407	339	387	1,12	0,99	0,86	0,99
										150	148	1,26	540	460	638	486	383	460	1,21	1,03	0,86	1,03
	$b_s=13$	940	495	95	2005,8	399,8	456,6	350	287	150	148	0,61	150	149	145	145	149	149	1,01	1,00	1,00	1,00
										250	233	0,79	250	222	237	237	222	222	1,07	0,95	0,95	0,95
										550	374	0,94	324	276	325	309	263	276	1,13	0,96	0,92	0,96
										750	429	1,17	439	360	490	407	317	360	1,18	0,96	0,85	0,96
										150	137	1,37	539	426	641	487	357	426	1,26	0,99	0,83	0,99
$b_w=110, b_i=10, b_s=5, t=1.0mm$	$b_s=17$	940	595	95	1890,2	500,6	460,1	350	322	150	149	0,55	150	150	145	145	150	150	1,01	1,01	1,01	1,01
										250	244	0,71	250	235	237	237	235	235	1,02	0,96	0,96	0,96
										550	446	0,84	325	299	324	308	285	299	1,01	0,93	0,88	0,93
										750	500	1,05	441	397	487	406	347	397	0,99	0,89	0,78	0,89
										150	122	1,22	541	473	635	485	393	473	1,08	0,95	0,79	0,95
	$b_s=19$	1400	275	80	658,2	107,2	104,4	350	152	150	101	1,18	113	98	136	106	83	98	1,12	0,97	0,82	0,97
										250	127	1,53	158	128	213	142	100	128	1,24	1,01	0,79	1,01
										550	185	1,81	196	151	280	170	113	151	1,29	0,99	0,74	0,99
										750	207	2,27	261	187	388	209	131	187	1,41	1,01	0,71	1,01
										150	2,65	318	215	466	235	144	215	153	1,04	0,70	1,04	1,04
$b_w=100, b_s=5, t=1.0mm$	$b_s=50$	1400	275	80	606,4	121,6	105,6	350	152	150	107	1,11	113	103	135	106	87	103	1,06	0,96	0,82	0,96
										250	129	1,43	158	136	210	142	106	136	1,23	1,05	0,82	1,05
										550	186	1,70	197	161	275	168	120	161	1,29	1,06	0,79	1,06
										750	206	2,13	262	200	376	206	139	200	1,41	1,07	0,75	1,07
										150	2,48	319	231	447	230	154	231	1,55	1,12	0,75	1,12	1,12
	$b_s=45$	1400	275	80	606,4	97,3	103,1	350	146	150	97	1,24	112	93	137	106	79	93	1,16	0,96	0,82	0,96
										250	118	1,60	157	122	215	142	96	122	1,33	1,03	0,81	1,03
										550	187	1,90	195	144	284	170	107	144	1,33	0,98	0,73	0,98
										750	207	2,38	260	177	396	211	124	177	1,39	0,95	0,66	0,95
										150	2,78	316	204	479	238	137	204	1,53	0,99	0,66	0,99	1,53
$b_w=80, b_s=10, t=1.3mm$	$b_s=115$	2400	540	95	342	128,6	126,8	350	145	150	110	1,08	121	106	125	107	93	106	1,10	0,96	0,84	0,96
										250	131	1,39	169	140	184	138	113	140	1,29	1,07	0,86	1,07
										550	169	1,65	210	166	228	159	127	151	1,45	1,14	0,88	1,04
										750	184	2,07	280	206	281	182	148	184	1,66	1,22	0,88	1,09
										150	2,41	341	238	300	190	164	211	1,85	1,29	0,89	1,15	1,85
	$b_s=100$	2400	530	90	267,9	132,0	137,0	350	152	150	112	1,07	124	107	119	106	95	107	1,10	0,95	0,85	0,95
										250	133	1,38	173	141	169	134	116	141	1,30	1,06	0,87	1,06
										550	176	1,63	216	168	203	151	131	152	1,42	1,10	0,86	1,00
										750	191	2,04	288	209	233	166	152	185	1,64	1,19	0,86	1,05
										150	2,38	351	241	235	166	168	211	1,84	1,26	0,88	1,10	1,84
$b_w=125$	$b_s=115$	2400	545	105	128,5	123,7	109,2	350	144	150	104	1,10	115	104	92	83	89	104	1,10	1,00	0,85	1,00
										250	125	1,42	160	137	111	94	108	137	1,28	1,10	0,86	1,10
										550	171	1,68	199	162	113	95	121	152	1,38	1,13	0,84	1,05
										750	187	2,11	265	202	113	95	141	186	1,55	1,18	0,83	1,09
										150	2,46	323	233	113	95	156	214	1,73	1,24	0,83	1,14	1,73

Table A4: H columns: SFEA ultimate strengths and corresponding DSM estimates (dimensions in mm, stresses in MPa) – IV

		GBT			SFEA			DSM												
		L	L <sub>cr.D</sub>	L <sub>cr.L</sub>	f <sub>E</sub>	f <sub>D</sub>	f <sub>L</sub>	f <sub>y</sub>	f <sub>U</sub>	λ <sub>D</sub>	f <sub>NL</sub>	f <sub>ND</sub>	f <sub>NE</sub>	f <sub>NLE</sub>	f <sub>NDL</sub>	f <sup>*</sup> <sub>NDL</sub>	f <sub>NL</sub> f <sub>U</sub>	f <sub>ND</sub> f <sub>U</sub>	f <sub>NDL</sub> f <sub>U</sub>	f <sup>*</sup> <sub>NDL</sub> f <sub>U</sub>
<i>b<sub>w</sub>=95, b<sub>i</sub>=80, t=0.95mm</i>	<i>b<sub>s</sub>=10</i>	2500	610	85	222,6	94,2	93,8	150	92,6	1,26	109	92	113	90	77	92	1,18	0,99	0,83	0,99
								250	106	1,63	152	120	156	112	93	99	1,43	1,13	0,87	0,93
								350	118	1,93	188	141	181	123	104	113	1,60	1,20	0,88	0,96
								550	145	2,42	251	174	195	129	120	134	1,73	1,20	0,83	0,92
								750	155	2,82	305	200	195	129	132	150	1,97	1,29	0,85	0,97
	<i>b<sub>s</sub>=9</i>	2500	570	85	226,1	89,0	93,6	150	83,8	1,30	109	90	114	91	75	90	1,30	1,07	0,90	1,07
								250	101	1,68	152	116	157	112	90	100	1,50	1,15	0,89	0,99
								350	113	1,98	188	137	183	124	101	114	1,67	1,21	0,89	1,01
								550	136	2,49	251	169	198	131	117	137	1,84	1,24	0,86	1,00
								750	144	2,90	305	194	198	131	128	154	2,12	1,35	0,89	1,07
<i>b<sub>w</sub>=150, b<sub>s</sub>=10, t=1.2mm</i>	<i>b<sub>s</sub>=11</i>	2500	655	85	219,1	100,1	94,0	150	101	1,22	109	95	113	90	79	95	1,08	0,94	0,78	0,94
								250	113	1,58	152	124	155	111	95	98	1,34	1,09	0,84	0,86
								350	123	1,87	189	146	179	122	107	110	1,53	1,18	0,87	0,90
								550	142	2,34	251	180	192	128	124	129	1,77	1,27	0,87	0,91
								750	161	2,74	305	207	192	128	136	143	1,90	1,29	0,85	0,89
	<i>b<sub>s</sub>=10</i>	1430	835	145	1804,5	53,8	53,8	150	62,9	1,67	90	70	145	88	54	64	1,42	1,11	0,86	1,01
								250	82	2,16	124	90	236	120	64	80	1,52	1,09	0,78	0,97
								350	99	2,55	154	105	323	146	71	92	1,55	1,06	0,72	0,93
								550	125	3,20	204	128	484	189	81	111	1,63	1,02	0,65	0,89
								750	148	3,73	248	146	630	222	89	126	1,67	0,99	0,60	0,85
<i>b<sub>w</sub>=150, b<sub>s</sub>=10, t=1.2mm</i>	<i>b<sub>s</sub>=130</i>	1430	795	140	1777,4	59,0	57,4	150	65,4	1,59	92	73	145	90	57	67	1,40	1,12	0,87	1,03
								250	86,3	2,06	127	94	236	123	68	84	1,47	1,09	0,78	0,98
								350	104	2,44	157	110	322	149	75	97	1,51	1,06	0,72	0,94
								550	132	3,05	209	135	483	193	86	118	1,58	1,02	0,65	0,89
								750	155	3,57	254	154	629	227	95	134	1,64	1,00	0,61	0,86
	<i>b<sub>s</sub>=140</i>	1430	870	155	1824,9	48,9	51,1	150	58,8	1,75	88	67	145	86	51	61	1,50	1,14	0,87	1,04
								250	77,1	2,26	122	85	236	118	60	76	1,58	1,10	0,78	0,99
								350	92,3	2,68	151	99	323	143	67	88	1,63	1,07	0,73	0,95
								550	118	3,35	200	121	485	185	77	106	1,70	1,03	0,65	0,90
								750	139	3,92	243	139	631	218	84	121	1,75	1,00	0,60	0,87
<i>b<sub>w</sub>=200, b<sub>s</sub>=190, t=1.5mm</i>	<i>b<sub>s</sub>=125</i>	1850	1105	200	1931,2	46,1	46,1	150	58,3	1,80	85	65	145	83	49	59	1,45	1,11	0,83	1,02
								250	75,6	2,33	117	82	237	113	57	74	1,55	1,09	0,76	0,98
								350	92,1	2,76	145	96	324	138	64	86	1,58	1,04	0,69	0,93
								550	117	3,45	193	117	488	179	73	103	1,65	1,00	0,62	0,88
								750	137	4,03	234	134	637	211	80	118	1,71	0,98	0,58	0,86
	<i>b<sub>s</sub>=14</i>	1850	1200	195	1915,2	38,3	45,6	150	57,6	1,98	84	59	145	83	44	52	1,47	1,02	0,77	0,90
								250	75,9	2,55	117	75	237	113	52	64	1,54	0,98	0,69	0,84
								350	91	3,02	145	87	324	138	58	73	1,59	0,95	0,64	0,80
								550	112	3,79	192	106	488	178	66	87	1,71	0,94	0,59	0,78
								750	131	4,43	233	121	637	210	72	99	1,78	0,92	0,55	0,75
<i>b<sub>w</sub>=200, b<sub>s</sub>=190, t=1.5mm</i>	<i>b<sub>s</sub>=145</i>	1850	1010	205	1946,1	52,8	46,5	150	59,3	1,69	85	69	145	83	52	66	1,43	1,17	0,88	1,11
								250	76,1	2,18	118	89	237	114	62	83	1,55	1,17	0,81	1,10
								350	89,9	2,57	146	103	325	139	68	97	1,62	1,15	0,76	1,08
								550	116	3,23	193	127	489	180	79	118	1,67	1,09	0,68	1,02
								750	135	3,77	234	145	638	212	86	134	1,74	1,07	0,64	1,00

Table A5: H columns: SFEA ultimate strengths and corresponding DSM estimates (dimensions in mm, stresses in MPa) – V

		GBT			SFEA			DSM																				
		L	L <sub>cr.D</sub>	L <sub>cr.L</sub>	f <sub>E</sub>	f <sub>D</sub>	f <sub>L</sub>	f <sub>y</sub>	f <sub>U</sub>	λ <sub>D</sub>	f <sub>NL</sub>	f <sub>ND</sub>	f <sub>NE</sub>	f <sub>NLE</sub>	f <sub>NDL</sub>	f <sup>*</sup> <sub>NDL</sub>	f <sub>NL</sub> f <sub>U</sub>	f <sub>ND</sub> f <sub>U</sub>	f <sub>NDL</sub> f <sub>U</sub>	f <sup>*</sup> <sub>NDL</sub> f <sub>U</sub>								
<i>b<sub>w</sub>=235, b<sub>l</sub>=160, t=1.9mm</i>	<i>b<sub>s</sub>=12.5</i>	1950	910	200	2206,9	65,3	64,5	150	76,3	1,52	96	77	146	94	61	75	1,25	1,01	0,80	0,99								
								250	99,1	1,96	133	99	238	129	73	96	1,34	1,00	0,73	0,97								
								350	117	2,32	164	116	328	158	81	112	1,40	0,99	0,69	0,96								
								550	144	2,90	219	142	496	205	93	137	1,52	0,99	0,65	0,95								
								750	169	3,39	265	163	651	243	102	157	1,57	0,97	0,60	0,93								
	<i>b<sub>s</sub>=14</i>	1950	985	200	2191,6	56,3	64,2	150	72,7	1,63	95	72	146	94	57	69	1,31	0,99	0,78	0,94								
								250	80,1	2,11	132	92	238	129	67	87	1,65	1,15	0,84	1,09								
								350	111	2,49	164	107	327	157	75	101	1,48	0,97	0,68	0,91								
								550	142	3,13	218	131	495	204	86	123	1,54	0,92	0,61	0,86								
								750	167	3,65	265	150	650	242	94	140	1,59	0,90	0,56	0,84								
<i>b<sub>w</sub>=150, b<sub>s</sub>=10, t=1.3mm</i>	<i>b<sub>s</sub>=11</i>	1950	830	200	2220,6	74,9	64,7	150	78,4	1,42	96	83	146	94	65	83	1,22	1,05	0,83	1,05								
								250	99,9	1,83	133	107	238	129	78	106	1,33	1,07	0,78	1,06								
								350	119	2,16	165	125	328	158	87	124	1,38	1,05	0,73	1,04								
								550	150	2,71	219	154	496	205	100	152	1,46	1,02	0,67	1,01								
								750	175	3,16	266	176	651	243	110	175	1,52	1,01	0,63	1,00								
	<i>b<sub>s</sub>=140</i>	900	800	150	4553,5	63,6	63,6	150	69,3	1,54	95	76	148	94	60	71	1,37	1,10	0,87	1,03								
								250	89	1,98	132	98	244	130	71	90	1,48	1,10	0,80	1,01								
								350	108	2,35	164	115	339	160	80	105	1,51	1,06	0,74	0,97								
								550	137	2,94	217	140	523	211	92	127	1,59	1,02	0,67	0,93								
								750	161	3,43	264	161	700	253	100	145	1,64	1,00	0,62	0,90								
<i>b<sub>w</sub>=150, b<sub>s</sub>=10, t=1.3mm</i>	<i>b<sub>s</sub>=130</i>	900	760	140	4484,8	71,6	67,9	150	73,2	1,45	97	81	148	96	64	81	1,33	1,10	0,88	1,10								
								250	95,8	1,87	135	104	244	133	77	95	1,41	1,09	0,80	1,00								
								350	114	2,21	167	122	339	164	85	111	1,47	1,07	0,75	0,97								
								550	144	2,77	223	150	522	216	98	135	1,55	1,04	0,68	0,93								
								750	169	3,24	270	172	699	259	108	153	1,60	1,02	0,64	0,91								
	<i>b<sub>s</sub>=150</i>	900	835	155	4605,1	58,3	58,3	150	65,8	1,60	92	73	148	91	57	68	1,40	1,11	0,86	1,03								
								250	85	2,07	128	93	244	126	67	86	1,51	1,10	0,79	1,01								
								350	96,1	2,45	158	109	339	155	75	99	1,65	1,14	0,78	1,03								
								550	131	3,07	210	134	523	204	86	120	1,61	1,02	0,66	0,92								
								750	154	3,59	255	153	701	245	94	137	1,66	0,99	0,61	0,89								
																	<i>Mean</i>	1,36	1,04	0,81	0,97							
																	<i>Sd.Dev.</i>	0,26	0,10	0,10	0,07							

## ANNEX B

Table B1: Z columns: SFEA ultimate strengths and corresponding DSM estimates (dimensions in *mm*, stresses in *MPa*) – I

		GBT			SFEA				DSM																																																																																																																																																																																																													
		L	L <sub>cr.D</sub>	L <sub>cr.L</sub>	f <sub>E</sub>	f <sub>D</sub>	f <sub>L</sub>	f <sub>y</sub>	f <sub>U</sub>	λ <sub>D</sub>	f <sub>NL</sub>	f <sub>ND</sub>	f <sub>NE</sub>	f <sub>NLE</sub>	f <sub>NDL</sub>	f <sup>*</sup> <sub>NDL</sub>	f <sub>NL</sub> / <sub>f<sub>U</sub></sub>	f <sub>ND</sub> / <sub>f<sub>U</sub></sub>	f <sub>NDL</sub> / <sub>f<sub>U</sub></sub>	f <sup>*</sup> <sub>NDL</sub> / <sub>f<sub>U</sub></sub>																																																																																																																																																																																																		
<i>b<sub>w</sub>=100, b<sub>s</sub>=100, t=1.9mm</i>	<i>b<sub>w</sub>=100, b<sub>s</sub>=100, t=1.0mm</i>	<i>b<sub>s</sub>=17.5</i>	<i>b<sub>s</sub>=20</i>	<i>b<sub>s</sub>=25</i>	<i>b<sub>s</sub>=30</i>	<i>b<sub>s</sub>=40</i>	<i>b<sub>s</sub>=50</i>	<i>b<sub>s</sub>=60</i>	<i>b<sub>s</sub>=70</i>	<i>b<sub>s</sub>=80</i>	<i>b<sub>s</sub>=90</i>	<i>b<sub>s</sub>=100</i>	<i>b<sub>s</sub>=110</i>	<i>b<sub>s</sub>=120</i>	<i>b<sub>s</sub>=130</i>	<i>b<sub>s</sub>=140</i>	<i>b<sub>s</sub>=150</i>	<i>b<sub>s</sub>=160</i>	<i>b<sub>s</sub>=170</i>	<i>b<sub>s</sub>=180</i>	<i>b<sub>s</sub>=190</i>	<i>b<sub>s</sub>=200</i>	<i>b<sub>s</sub>=210</i>	<i>b<sub>s</sub>=220</i>	<i>b<sub>s</sub>=230</i>	<i>b<sub>s</sub>=240</i>	<i>b<sub>s</sub>=250</i>	<i>b<sub>s</sub>=260</i>	<i>b<sub>s</sub>=270</i>	<i>b<sub>s</sub>=280</i>	<i>b<sub>s</sub>=290</i>	<i>b<sub>s</sub>=300</i>	<i>b<sub>s</sub>=310</i>	<i>b<sub>s</sub>=320</i>	<i>b<sub>s</sub>=330</i>	<i>b<sub>s</sub>=340</i>	<i>b<sub>s</sub>=350</i>	<i>b<sub>s</sub>=360</i>	<i>b<sub>s</sub>=370</i>	<i>b<sub>s</sub>=380</i>	<i>b<sub>s</sub>=390</i>	<i>b<sub>s</sub>=400</i>	<i>b<sub>s</sub>=410</i>	<i>b<sub>s</sub>=420</i>	<i>b<sub>s</sub>=430</i>	<i>b<sub>s</sub>=440</i>	<i>b<sub>s</sub>=450</i>	<i>b<sub>s</sub>=460</i>	<i>b<sub>s</sub>=470</i>	<i>b<sub>s</sub>=480</i>	<i>b<sub>s</sub>=490</i>	<i>b<sub>s</sub>=500</i>	<i>b<sub>s</sub>=510</i>	<i>b<sub>s</sub>=520</i>	<i>b<sub>s</sub>=530</i>	<i>b<sub>s</sub>=540</i>	<i>b<sub>s</sub>=550</i>	<i>b<sub>s</sub>=560</i>	<i>b<sub>s</sub>=570</i>	<i>b<sub>s</sub>=580</i>	<i>b<sub>s</sub>=590</i>	<i>b<sub>s</sub>=600</i>	<i>b<sub>s</sub>=610</i>	<i>b<sub>s</sub>=620</i>	<i>b<sub>s</sub>=630</i>	<i>b<sub>s</sub>=640</i>	<i>b<sub>s</sub>=650</i>	<i>b<sub>s</sub>=660</i>	<i>b<sub>s</sub>=670</i>	<i>b<sub>s</sub>=680</i>	<i>b<sub>s</sub>=690</i>	<i>b<sub>s</sub>=700</i>	<i>b<sub>s</sub>=710</i>	<i>b<sub>s</sub>=720</i>	<i>b<sub>s</sub>=730</i>	<i>b<sub>s</sub>=740</i>	<i>b<sub>s</sub>=750</i>	<i>b<sub>s</sub>=760</i>	<i>b<sub>s</sub>=770</i>	<i>b<sub>s</sub>=780</i>	<i>b<sub>s</sub>=790</i>	<i>b<sub>s</sub>=800</i>	<i>b<sub>s</sub>=810</i>	<i>b<sub>s</sub>=820</i>	<i>b<sub>s</sub>=830</i>	<i>b<sub>s</sub>=840</i>	<i>b<sub>s</sub>=850</i>	<i>b<sub>s</sub>=860</i>	<i>b<sub>s</sub>=870</i>	<i>b<sub>s</sub>=880</i>	<i>b<sub>s</sub>=890</i>	<i>b<sub>s</sub>=900</i>	<i>b<sub>s</sub>=910</i>	<i>b<sub>s</sub>=920</i>	<i>b<sub>s</sub>=930</i>	<i>b<sub>s</sub>=940</i>	<i>b<sub>s</sub>=950</i>	<i>b<sub>s</sub>=960</i>	<i>b<sub>s</sub>=970</i>	<i>b<sub>s</sub>=980</i>	<i>b<sub>s</sub>=990</i>	<i>b<sub>s</sub>=1000</i>	<i>b<sub>s</sub>=1010</i>	<i>b<sub>s</sub>=1020</i>	<i>b<sub>s</sub>=1030</i>	<i>b<sub>s</sub>=1040</i>	<i>b<sub>s</sub>=1050</i>	<i>b<sub>s</sub>=1060</i>	<i>b<sub>s</sub>=1070</i>	<i>b<sub>s</sub>=1080</i>	<i>b<sub>s</sub>=1090</i>	<i>b<sub>s</sub>=1100</i>	<i>b<sub>s</sub>=1110</i>	<i>b<sub>s</sub>=1120</i>	<i>b<sub>s</sub>=1130</i>	<i>b<sub>s</sub>=1140</i>	<i>b<sub>s</sub>=1150</i>	<i>b<sub>s</sub>=1160</i>	<i>b<sub>s</sub>=1170</i>	<i>b<sub>s</sub>=1180</i>	<i>b<sub>s</sub>=1190</i>	<i>b<sub>s</sub>=1200</i>	<i>b<sub>s</sub>=1210</i>	<i>b<sub>s</sub>=1220</i>	<i>b<sub>s</sub>=1230</i>	<i>b<sub>s</sub>=1240</i>	<i>b<sub>s</sub>=1250</i>	<i>b<sub>s</sub>=1260</i>	<i>b<sub>s</sub>=1270</i>	<i>b<sub>s</sub>=1280</i>	<i>b<sub>s</sub>=1290</i>	<i>b<sub>s</sub>=1300</i>	<i>b<sub>s</sub>=1310</i>	<i>b<sub>s</sub>=1320</i>	<i>b<sub>s</sub>=1330</i>	<i>b<sub>s</sub>=1340</i>	<i>b<sub>s</sub>=1350</i>	<i>b<sub>s</sub>=1360</i>	<i>b<sub>s</sub>=1370</i>	<i>b<sub>s</sub>=1380</i>	<i>b<sub>s</sub>=1390</i>	<i>b<sub>s</sub>=1400</i>	<i>b<sub>s</sub>=1410</i>	<i>b<sub>s</sub>=1420</i>	<i>b<sub>s</sub>=1430</i>	<i>b<sub>s</sub>=1440</i>	<i>b<sub>s</sub>=1450</i>	<i>b<sub>s</sub>=1460</i>	<i>b<sub>s</sub>=1470</i>	<i>b<sub>s</sub>=1480</i>	<i>b<sub>s</sub>=1490</i>	<i>b<sub>s</sub>=1500</i>	<i>b<sub>s</sub>=1510</i>	<i>b<sub>s</sub>=1520</i>	<i>b<sub>s</sub>=1530</i>	<i>b<sub>s</sub>=1540</i>	<i>b<sub>s</sub>=1550</i>	<i>b<sub>s</sub>=1560</i>	<i>b<sub>s</sub>=1570</i>	<i>b<sub>s</sub>=1580</i>	<i>b<sub>s</sub>=1590</i>	<i>b<sub>s</sub>=1600</i>	<i>b<sub>s</sub>=1610</i>	<i>b<sub>s</sub>=1620</i>	<i>b<sub>s</sub>=1630</i>	<i>b<sub>s</sub>=1640</i>	<i>b<sub>s</sub>=1650</i>	<i>b<sub>s</sub>=1660</i>	<i>b<sub>s</sub>=1670</i>	<i>b<sub>s</sub>=1680</i>	<i>b<sub>s</sub>=1690</i>	<i>b<sub>s</sub>=1700</i>	<i>b<sub>s</sub>=1710</i>	<i>b<sub>s</sub>=1720</i>	<i>b<sub>s</sub>=1730</i>	<i>b<sub>s</sub>=1740</i>	<i>b<sub>s</sub>=1750</i>	<i>b<sub>s</sub>=1760</i>	<i>b<sub>s</sub>=1770</i>	<i>b<sub>s</sub>=1780</i>	<i>b<sub>s</sub>=1790</i>	<i>b<sub>s</sub>=1800</i>	<i>b<sub>s</sub>=1810</i>	<i>b<sub>s</sub>=1820</i>	<i>b<sub>s</sub>=1830</i>	<i>b<sub>s</sub>=1840</i>	<i>b<sub>s</sub>=1850</i>	<i>b<sub>s</sub>=1860</i>	<i>b<sub>s</sub>=1870</i>	<i>b<sub>s</sub>=1880</i>	<i>b<sub>s</sub>=1890</i>	<i>b<sub>s</sub>=1900</i>	<i>b<sub>s</sub>=1910</i>	<i>b<sub>s</sub>=1920</i>	<i>b<sub>s</sub>=1930</i>	<i>b<sub>s</sub>=1940</i>	<i>b<sub>s</sub>=1950</i>	<i>b<sub>s</sub>=1960</i>	<i>b<sub>s</sub>=1970</i>	<i>b<sub>s</sub>=1980</i>	<i>b<sub>s</sub>=1990</i>	<i>b<sub>s</sub>=2000</i>	<i>b<sub>s</sub>=2010</i>	<i>b<sub>s</sub>=2020</i>	<i>b<sub>s</sub>=2030</i>	<i>b<sub>s</sub>=2040</i>	<i>b<sub>s</sub>=2050</i>	<i>b<sub>s</sub>=2060</i>	<i>b<sub>s</sub>=2070</i>	<i>b<sub>s</sub>=2080</i>	<i>b<sub>s</sub>=2090</i>	<i>b<sub>s</sub>=2100</i>	<i>b<sub>s</sub>=2110</i>	<i>b<sub>s</sub>=2120</i>

Table B2: Z columns: SFEA ultimate strengths and corresponding DSM estimates (dimensions in  $mm$ , stresses in  $MPa$ ) – II

			GBT			SFEA			DSM													
		L	$L_{cr,D}$	$L_{cr,L}$	$f_E$	$f_D$	$f_L$	$f_y$	$f_U$	$\lambda_D$	$f_{NL}$	$f_{ND}$	$f_{NE}$	$f_{NLE}$	$f_{NDL}$	$f^{*}_{NDL}$	$\frac{f_{NL}}{f_U}$	$\frac{f_{ND}}{f_U}$	$\frac{f_{NDL}}{f_U}$	$\frac{f^{*}_{NDL}}{f_U}$		
$b_w=100, b_s=10, t=2.4mm$	$b_l=55$	620	595	85	468,2	103,9	103,8	350	122	150	96,6	1,20	113	96	131	103	82	96	1,17	1,00	0,85	1,00
										250	112	1,55	157	126	200	136	99	106	1,40	1,12	0,88	0,95
										184	195	149	256	160	111	122			1,60	1,22	0,91	1,00
										550	157	2,30	261	184	336	190	128	145	1,66	1,17	0,82	0,92
										750	179	2,69	317	212	384	207	142	163	1,77	1,18	0,79	0,91
	$b_l=60$	620	585	85	432,5	107,2	114,6	350	126	150	98,8	1,18	117	98	130	106	84	98	1,18	0,99	0,86	0,99
										250	117	1,53	163	128	196	139	102	110	1,39	1,09	0,87	0,94
										181	202	151	249	163	115	126			1,61	1,20	0,91	1,00
										550	152	2,27	270	187	323	192	133	151	1,78	1,23	0,87	0,99
										750	175	2,65	329	215	363	207	146	170	1,88	1,23	0,84	0,97
$b_w=100, b_s=10, t=1.9mm$	$b_l=60$	620	600	90	512,9	99,4	88,9	350	122	150	92,5	1,23	107	94	133	99	78	94	1,16	1,02	0,84	1,02
										250	109	1,59	149	123	204	131	94	105	1,37	1,13	0,86	0,96
										188	185	145	263	154	105	121			1,51	1,19	0,86	0,99
										550	145	2,35	246	179	351	185	122	145	1,70	1,24	0,84	1,00
										750	167	2,75	299	207	407	203	135	163	1,79	1,24	0,81	0,98
	$b_l=110$	1030	500	95	2584,1	171,0	171,6	350	178	150	129	0,94	133	118	146	131	110	118	1,03	0,92	0,85	0,92
										250	168	1,21	187	159	240	182	135	159	1,11	0,95	0,81	0,95
										1,43	233	191	331	225	154	191			1,31	1,07	0,86	1,07
										550	229	1,79	313	239	503	295	180	222	1,37	1,04	0,79	0,97
										750	261	2,09	381	277	664	353	199	256	1,46	1,06	0,76	0,98
$b_w=180, b_s=10, t=1.9mm$	$b_l=130$	1030	505	100	2675,7	162,9	156,8	350	184	150	128	0,96	129	116	147	127	106	116	1,01	0,91	0,83	0,91
										250	163	1,24	182	156	240	177	130	156	1,11	0,96	0,80	0,96
										1,47	226	186	331	218	148	186			1,23	1,01	0,80	1,01
										550	222	1,84	303	233	505	286	173	219	1,36	1,05	0,78	0,99
										750	260	2,15	369	270	667	342	191	252	1,42	1,04	0,74	0,97
	$b_l=110$	1030	495	95	2443,4	177,4	194,0	350	196	150	131	0,92	139	120	146	136	114	120	1,06	0,92	0,87	0,92
										250	176	1,19	195	162	240	190	141	162	1,11	0,92	0,80	0,92
										1,40	244	194	330	234	160	194			1,24	0,99	0,82	0,99
										550	233	1,76	327	244	501	307	187	228	1,40	1,05	0,80	0,98
										750	269	2,06	399	283	660	367	208	263	1,48	1,05	0,77	0,98
$b_w=180, b_s=20, t=4.0mm$	$b_l=100$	2000	615	150	1647,3	483,1	498,6	350	342	150	149	0,56	150	150	144	144	150	150	1,01	1,01	1,01	1,01
										250	247	0,72	250	233	235	235	233	233	1,01	0,94	0,94	0,94
										0,85	334	296	320	314	287	296			0,98	0,87	0,84	0,87
										550	459	1,07	453	391	478	412	348	391	0,99	0,85	0,76	0,85
										750	510	1,25	556	465	620	490	394	465	1,09	0,91	0,77	0,91
	$b_l=90$	2000	570	145	1419,0	530,6	504,6	350	344	150	149	0,53	150	150	144	144	150	150	1,01	1,01	1,01	1,01
										250	248	0,69	250	238	232	232	238	238	1,01	0,96	0,96	0,96
										0,81	335	305	316	312	296	305			0,97	0,89	0,86	0,89
										550	480	1,02	454	407	468	408	362	407	0,95	0,85	0,75	0,85
										750	568	1,19	558	486	601	482	410	486	0,98	0,85	0,72	0,85
$b_w=180, b_s=20, t=4.0mm$	$b_l=110$	2000	655	150	1867,8	439,6	491,9	350	332	150	149	0,58	150	150	145	145	150	150	1,01	1,00	1,00	1,00
										250	246	0,75	250	228	236	236	228	228	1,02	0,93	0,93	0,93
										0,89	332	286	324	315	277	286			1,00	0,86	0,83	0,86
										550	432	1,12	451	376	486	415	335	376	1,04	0,87	0,77	0,87
										750	463	1,31	553	446	634	495	377	446	1,19	0,96	0,81	0,96

Table B3: Z columns: SFEA ultimate strengths and corresponding DSM estimates (dimensions in mm, stresses in MPa) – III

		GBT			SFEA			DSM														
		L	L <sub>cr.D</sub>	L <sub>cr.L</sub>	f <sub>E</sub>	f <sub>D</sub>	f <sub>L</sub>	f <sub>y</sub>	f <sub>U</sub>	λ <sub>D</sub>	f <sub>NL</sub>	f <sub>ND</sub>	f <sub>NE</sub>	f <sub>NLE</sub>	f <sub>NDL</sub>	f <sup>*</sup> <sub>NDL</sub>	f <sub>NL</sub> / <sub>f<sub>U</sub></sub>	f <sub>ND</sub> / <sub>f<sub>U</sub></sub>	f <sub>NDL</sub> / <sub>f<sub>U</sub></sub>	f <sup>*</sup> <sub>NDL</sub> / <sub>f<sub>U</sub></sub>		
<i>b<sub>w</sub>=110, b<sub>s</sub>=85, t=2.4mm</i>	<i>b<sub>s</sub>=15</i>	940	540	95	4246,8	457,5	457,3	350	325	150	148	0,57	150	150	148	148	150	150	1,01	1,01	1,01	1,01
										250	243	0,74	250	230	244	244	230	230	1,03	0,95	0,95	0,95
										350	325	0,87	324	290	338	317	276	290	1,00	0,89	0,85	0,89
										550	427	1,10	440	382	521	424	335	382	1,03	0,90	0,78	0,90
										750	472	1,28	540	454	697	514	378	454	1,14	0,96	0,80	0,96
	<i>b<sub>s</sub>=13</i>	940	490	100	4156,3	380,5	454,7	350	305	150	148	0,63	150	148	148	148	148	148	1,01	1,00	1,00	1,00
										250	241	0,81	250	218	244	244	218	218	1,04	0,91	0,91	0,91
										350	305	0,96	324	271	338	316	259	271	1,06	0,89	0,85	0,89
										550	377	1,20	439	353	520	423	310	353	1,16	0,94	0,82	0,94
										750	403	1,40	539	416	695	512	348	416	1,34	1,03	0,86	1,03
<i>b<sub>w</sub>=100, b<sub>s</sub>=5, t=1.0mm</i>	<i>b<sub>s</sub>=17</i>	940	590	95	4337,9	522,9	458,9	350	332	150	148	0,54	150	150	148	148	150	150	1,01	1,01	1,01	1,01
										250	245	0,69	250	238	244	244	238	238	1,02	0,97	0,97	0,97
										350	332	0,82	325	304	338	317	288	304	0,98	0,91	0,87	0,91
										550	461	1,03	440	404	522	425	353	404	0,95	0,88	0,77	0,88
										750	513	1,20	540	482	698	515	400	482	1,05	0,94	0,78	0,94
	<i>b<sub>s</sub>=10</i>	1400	270	80	777,9	105,1	104,1	350	151	150	101	1,19	113	97	138	107	82	97	1,12	0,96	0,81	0,96
										250	126	1,54	157	127	219	144	99	127	1,25	1,00	0,79	1,00
										350	151	1,82	196	149	290	173	112	149	1,30	0,99	0,74	0,99
										550	185	2,29	261	185	409	216	129	185	1,41	1,00	0,70	1,00
										750	207	2,67	317	213	501	246	142	213	1,53	1,03	0,69	1,03
<i>b<sub>w</sub>=80, b<sub>s</sub>=10, t=1.3mm</i>	<i>b<sub>s</sub>=45</i>	1400	250	80	653,5	116,3	105,2	350	151	150	107	1,14	113	101	136	106	86	101	1,06	0,95	0,80	0,95
										250	129	1,47	158	133	213	142	104	133	1,23	1,03	0,81	1,03
										350	151	1,73	196	157	280	170	117	157	1,30	1,04	0,78	1,04
										550	186	2,17	262	195	387	209	136	195	1,41	1,05	0,73	1,05
										750	206	2,54	318	225	464	235	150	225	1,55	1,09	0,73	1,09
	<i>b<sub>s</sub>=55</i>	1400	290	85	903,2	95,0	102,8	350	145	150	97	1,26	112	92	140	107	79	92	1,16	0,95	0,81	0,95
										250	123	1,62	157	120	223	145	95	120	1,27	0,98	0,77	0,98
										350	145	1,92	195	142	298	175	106	142	1,34	0,98	0,73	0,98
										550	186	2,41	260	175	426	221	123	175	1,40	0,94	0,66	0,94
										750	208	2,81	316	201	530	254	135	201	1,52	0,97	0,65	0,97
<i>b<sub>w</sub>=125</i>	<i>b<sub>s</sub>=15</i>	2400	535	95	597,0	126,5	126,6	350	150	150	120	1,09	121	105	135	112	92	105	1,00	0,87	0,77	0,87
										250	131	1,41	169	139	210	150	112	139	1,29	1,06	0,86	1,06
										350	150	1,66	210	164	274	179	126	150	1,40	1,10	0,84	1,00
										550	177	2,09	280	204	374	219	147	184	1,58	1,15	0,83	1,04
										750	192	2,43	341	236	443	244	162	210	1,78	1,23	0,84	1,09
	<i>b<sub>s</sub>=105</i>	2400	545	105	629,9	120,3	109,0	350	144	150	118	1,12	115	103	136	107	88	103	0,97	0,87	0,74	0,87
										250	130	1,44	160	135	212	144	106	135	1,23	1,04	0,82	1,04
										350	144	1,71	199	160	277	171	120	150	1,38	1,11	0,83	1,04
										550	165	2,14	265	199	382	210	139	184	1,61	1,20	0,84	1,11
										750	195	2,50	323	229	456	235	154	211	1,65	1,18	0,79	1,08

Table B4: Z columns: SFEA ultimate strengths and corresponding DSM estimates (dimensions in *mm*, stresses in *MPa*) – IV

			GBT			SFEA			DSM													
		L	L <sub>cr.D</sub>	L <sub>cr.L</sub>	f <sub>E</sub>	f <sub>D</sub>	f <sub>L</sub>	f <sub>y</sub>	f <sub>U</sub>	λ <sub>D</sub>	f <sub>NL</sub>	f <sub>ND</sub>	f <sub>NE</sub>	f <sub>NLE</sub>	f <sub>NDL</sub>	f <sup>*</sup> <sub>NDL</sub>	f <sub>NL</sub> f <sub>U</sub>	f <sub>ND</sub> f <sub>U</sub>	f <sub>NDL</sub> f <sub>U</sub>	f <sup>*</sup> <sub>NDL</sub> f <sub>U</sub>		
<i>b<sub>w</sub>=95, b=80, t=0.95mm</i>	<i>b<sub>s</sub>=10</i>	2500	610	85	468,2	98,7	93,8	350	114	150	100	1,23	109	94	131	100	78	94	1,09	0,94	0,78	0,94
										250	107	1,59	152	123	200	131	95	101	1,42	1,15	0,88	0,95
										188	188	145	256	154	106	115			1,65	1,27	0,93	1,01
										550	121	2,36	251	179	336	184	123	137	2,07	1,48	1,02	1,13
										750	163	2,76	305	206	384	200	135	154	1,87	1,26	0,83	0,94
	<i>b<sub>s</sub>=9</i>	2500	565	85	502,3	88,0	93,5	350	112	150	89,4	1,31	109	89	132	100	75	89	1,22	1,00	0,84	1,00
										250	101	1,69	152	116	203	132	90	99	1,50	1,15	0,89	0,98
										550	126	1,99	188	136	261	156	100	114	1,68	1,22	0,90	1,02
										750	147	2,50	251	168	348	187	116	137	1,99	1,33	0,92	1,08
										2,92	305	193	401	205	127	154			2,07	1,31	0,87	1,05
<i>b<sub>w</sub>=150, b<sub>s</sub>=10, t=1.2mm</i>	<i>b<sub>s</sub>=11</i>	2500	650	85	473,5	106,3	94,0	350	124	150	111	1,19	109	97	131	100	81	97	0,98	0,88	0,73	0,88
										250	116	1,53	152	127	200	132	98	101	1,31	1,10	0,84	0,87
										550	129	1,81	189	150	257	155	110	114	1,52	1,21	0,89	0,92
										750	149	2,27	251	186	338	184	128	134	1,95	1,44	0,99	1,04
										2,66	305	214	386	201	141	149			2,05	1,44	0,94	1,00
	<i>b<sub>s</sub>=140</i>	1430	830	145	3753,8	53,7	53,7	350	105	150	67,4	1,67	90	70	148	89	54	64	1,33	1,04	0,80	0,94
										250	76,8	2,16	124	89	243	122	64	80	1,62	1,17	0,83	1,04
										550	126	2,55	154	104	337	150	71	92	1,46	0,99	0,68	0,88
										750	148	3,20	204	128	517	196	81	111	1,62	1,01	0,65	0,88
										2,74	248	146	690	235	89	126			1,67	0,99	0,60	0,85
<i>b<sub>w</sub>=150, b<sub>s</sub>=10, t=1.2mm</i>	<i>b<sub>s</sub>=130</i>	1430	790	140	3514,6	58,8	57,4	350	102	150	61,6	1,60	92	73	147	91	57	67	1,49	1,19	0,92	1,09
										250	86,4	2,06	127	94	243	125	67	84	1,47	1,09	0,78	0,98
										550	113	2,44	157	110	336	153	75	98	1,54	1,08	0,74	0,96
										750	131	3,06	209	134	515	201	86	118	1,85	1,19	0,76	1,04
										2,57	254	154	686	240	95	134			1,94	1,18	0,72	1,02
	<i>b<sub>s</sub>=150</i>	1430	865	155	3966,8	48,8	51,0	350	96,7	150	58,3	1,75	88	67	148	87	51	61	1,51	1,14	0,87	1,05
										250	80,7	2,26	122	85	243	120	60	76	1,51	1,05	0,75	0,95
										550	120	2,68	151	99	337	147	67	88	1,56	1,02	0,69	0,91
										750	145	3,36	200	121	519	193	77	107	1,67	1,01	0,64	0,89
										2,92	243	139	693	231	84	121			1,67	0,96	0,58	0,83
<i>b<sub>w</sub>=200, b<sub>s</sub>=190, t=1.5mm</i>	<i>b<sub>s</sub>=125</i>	1850	1105	200	4031,1	46,0	46,0	350	84,2	150	58,3	1,81	85	65	148	84	49	59	1,45	1,11	0,83	1,02
										250	72,1	2,33	117	82	244	115	57	74	1,63	1,14	0,80	1,03
										550	117	2,76	145	96	338	142	64	86	1,72	1,14	0,76	1,02
										750	137	3,46	193	117	519	186	73	103	1,65	1,00	0,62	0,88
										2,04	233	134	694	222	80	117			1,70	0,98	0,58	0,86
	<i>b<sub>s</sub>=14</i>	1850	1195	195	4058,6	38,1	45,6	350	90,9	150	57,5	1,98	84	59	148	84	44	52	1,47	1,02	0,77	0,90
										250	75,6	2,56	117	74	244	115	52	64	1,55	0,98	0,69	0,84
										550	112	3,03	145	86	338	141	58	73	1,59	0,95	0,63	0,80
										750	133	3,80	192	105	520	185	66	87	1,71	0,94	0,59	0,78
										2,44	233	120	694	222	72	99			1,75	0,90	0,54	0,74
<i>b<sub>s</sub>=11</i>	1850	1010	205	4003,5	52,5	46,5	350	91,4	150	59,2	1,69	85	69	148	84	52	66	1,44	1,17	0,87	1,11	
									250	76,2	2,18	118	88	244	116	61	83	1,55	1,16	0,81	1,09	
									550	116	2,58	146	103	337	142	68	97	1,59	1,13	0,75	1,06	
									750	135	3,24	193	126	519	186	78	117	1,67	1,09	0,68	1,01	
									2,78	234	144	693	223	86	134			1,74	1,07	0,64	0,99	

Table B5: Z columns: SFEA ultimate strengths and corresponding DSM estimates (dimensions in  $mm$ , stresses in  $MPa$ ) – V

			GBT			SFEA			DSM																					
		L	$L_{cr,D}$	$L_{cr,L}$	$f_E$	$f_D$	$f_L$	$f_y$	$f_U$	$\lambda_D$	$f_{NL}$	$f_{ND}$	$f_{NE}$	$f_{NLE}$	$f_{NDL}$	$f^{*}_{NDL}$	$\frac{f_{NL}}{f_U}$	$\frac{f_{ND}}{f_U}$	$\frac{f_{NDL}}{f_U}$	$\frac{f^{*}_{NDL}}{f_U}$										
$b_w=235, b_s=160, t=1.9mm$	$b_s=12.5$	1950	905	200	3489,5	64,3	64,3	350	117	150	72,8	1,53	95	77	147	94	60	75	1,31	1,05	0,83	1,03								
										250	98,7	1,97	133	98	243	130	72	95	1,34	1,00	0,73	0,97								
										550	144	2,33	164	115	336	160	80	111	1,40	0,98	0,69	0,95								
										750	169	2,92	218	141	515	209	92	136	1,52	0,98	0,64	0,95								
										3,42	265	162	685	251	101	156			1,57	0,96	0,60	0,92								
	$b_s=14$	1950	980	200	3526,5	55,7	64,1	350	111	150	71,9	1,64	95	71	147	94	57	68	1,33	0,99	0,79	0,95								
										250	81,6	2,12	132	91	243	130	67	87	1,62	1,12	0,82	1,06								
										550	145	3,14	218	130	515	209	86	122	1,48	0,96	0,67	0,91								
										750	170	3,67	265	149	686	250	94	139	1,56	0,88	0,55	0,82								
										150	83,6	1,42	96	82	147	95	64	82	1,14	0,98	0,77	0,98								
$b_w=150, b_s=10, t=1.3mm$	$b_s=11$	1950	830	205	3452,1	73,9	64,6	350	115	250	100	1,84	133	106	243	130	77	106	1,33	1,06	0,77	1,06								
										550	155	2,18	164	124	335	160	86	124	1,43	1,08	0,75	1,08								
										750	185	2,73	219	153	515	210	99	152	1,41	0,98	0,64	0,98								
										150	83,6	3,19	265	175	685	251	109	174	1,43	0,95	0,59	0,94								
										250	100	1,54	95	76	149	95	60	71	1,37	1,10	0,86	1,03								
	$b_s=140$	900	800	150	9476,9	63,5	63,5	350	108	550	137	1,98	132	98	247	131	71	90	1,45	1,08	0,79	0,99								
										750	161	2,35	163	114	345	162	80	104	1,51	1,06	0,74	0,97								
										150	69,4	2,94	217	140	537	214	91	127	1,59	1,02	0,67	0,93								
										250	90,9	3,44	264	161	726	258	100	144	1,64	1,00	0,62	0,90								
										750	175,7	1,42	97	82	149	97	65	82	1,28	1,09	0,86	1,09								
$b_w=150, b_s=10, t=1.3mm$	$b_s=130$	900	755	140	8872,9	74,7	67,8	350	131	150	75,7	1,83	135	106	247	134	78	98	1,38	1,09	0,80	1,00								
										250	97,9	2,16	167	125	344	166	87	114	1,28	0,95	0,67	0,87								
										550	166	2,71	223	153	536	219	101	138	1,34	0,92	0,61	0,83								
										750	192	3,17	270	176	724	264	111	158	1,41	0,92	0,58	0,82								
										150	69,7	1,61	92	73	149	92	57	68	1,32	1,05	0,81	0,97								
	$b_s=150$	900	835	155	10014,6	58,2	58,2	350	110	250	91,2	2,07	128	93	247	127	67	86	1,40	1,02	0,74	0,94								
										550	140	2,45	158	109	345	157	75	99	1,44	0,99	0,68	0,90								
										750	165	3,07	210	134	538	207	86	120	1,50	0,95	0,61	0,86								
										150	69,7	3,59	255	153	727	250	94	137	1,55	0,93	0,57	0,83								
										250	91,2																			
												<i>Mean</i>		1,34		1,03		0,80		0,96										
												<i>Sd.Dev.</i>		0,27		0,11		0,11		0,07										

## ANNEX C

Table C1: C columns: SFEA ultimate strengths and corresponding DSM estimates (dimensions in  $mm$ , stresses in  $MPa$ ) – I

		GBT			SFEA				DSM											
		L	$L_{cr.D}$	$L_{cr.L}$	$f_E$	$f_D$	$f_L$	$f_y$	$f_U$	$\lambda_D$	$f_{NL}$	$f_{ND}$	$f_{NE}$	$f_{NLE}$	$f_{NDL}$	$f^*_{NDL}$	$\frac{f_{NL}}{f_U}$	$\frac{f_{ND}}{f_U}$	$\frac{f_{NDL}}{f_U}$	$\frac{f^*_{NDL}}{f_U}$
$b_w=100, b_s=100, t=1.9mm$	$b_s=17.5$	1760	310    85    4305,6	564,2    583,6	150	149	0,52	150	150	148	148	150	150	150	1,01	1,01	1,01	1,01		
					250	245	0,67	250	241	244	244	241	241	241	1,02	0,99	0,99	0,99		
					350	335	0,79	350	311	338	338	311	311	311	1,04	0,93	0,93	0,93		
					550	456	0,99	477	417	521	460	382	417	417	1,05	0,91	0,84	0,91		
					750	538	1,15	586	499	697	559	433	499	499	1,09	0,93	0,80	0,93		
	$b_s=20$	1760	290    80    4110,1	589,9    591,0	150	149	0,50	150	150	148	148	150	150	150	1,01	1,01	1,01	1,01		
					250	246	0,65	250	243	244	244	243	243	243	1,02	0,99	0,99	0,99		
					350	338	0,77	350	315	338	338	315	315	315	1,04	0,93	0,93	0,93		
					550	473	0,97	479	424	520	461	389	424	424	1,01	0,90	0,82	0,90		
					750	553	1,13	589	509	695	560	442	509	509	1,06	0,92	0,80	0,92		
$b_w=100, b_s=10, t=1.0mm$	$b_s=16$	1760	325    85    4460,7	529,3    579,2	150	149	0,53	150	150	148	148	150	150	150	1,01	1,01	1,01	1,01		
					250	244	0,69	250	238	244	244	238	238	238	1,02	0,98	0,98	0,98		
					350	329	0,81	350	305	339	339	305	305	305	1,06	0,93	0,93	0,93		
					550	440	1,02	476	406	522	459	372	406	406	1,08	0,92	0,85	0,92		
					750	520	1,19	585	485	699	558	421	485	485	1,12	0,93	0,81	0,93		
	$b_w=20$	2500	590    150    4808,0	112,7    112,7	150	104	1,15	116	100	148	115	86	100	100	1,11	0,96	0,83	0,96		
					250	132	1,49	162	131	245	160	104	131	131	1,23	0,99	0,79	0,99		
					350	156	1,76	201	155	339	197	117	155	155	1,29	0,99	0,75	0,99		
					550	195	2,21	269	192	524	260	136	192	192	1,38	0,98	0,70	0,98		
					750	230	2,58	327	221	703	314	150	221	221	1,42	0,96	0,65	0,96		
$b_l=80, b_s=10, t=1.0mm$	$b_w=95$	2500	650    160    5116,1	98,8    108,5	150	96,6	1,23	114	94	148	113	81	94	94	1,18	0,97	0,84	0,97		
					250	122	1,59	160	123	245	158	97	122	122	1,31	1,01	0,80	1,00		
					350	145	1,88	199	145	340	195	109	144	144	1,37	1,00	0,75	0,99		
					550	184	2,36	265	179	526	257	126	178	178	1,44	0,97	0,69	0,97		
					750	218	2,76	322	206	705	310	139	205	205	1,48	0,94	0,64	0,94		
	$b_w=88$	2500	515    145    4306,6	131,6    116,0	150	116	1,07	117	107	148	116	92	107	107	1,01	0,92	0,79	0,92		
					250	147	1,38	164	141	244	161	112	141	141	1,11	0,96	0,76	0,96		
					350	175	1,63	203	168	338	199	126	168	168	1,16	0,96	0,72	0,96		
					550	223	2,04	271	208	521	262	147	208	208	1,22	0,93	0,66	0,93		
					750	261	2,39	330	241	697	315	163	241	241	1,27	0,92	0,62	0,92		
$b_l=80, b_s=10, t=1.5mm$	$b_w=105$	1150	755    105    823,2	261,5    261,5	150	145	0,76	150	136	139	139	136	136	136	1,03	0,94	0,94	0,94		
					250	198	0,98	216	191	220	198	174	191	191	1,09	0,96	0,88	0,96		
					350	239	1,16	270	232	293	240	200	232	232	1,13	0,97	0,84	0,97		
					550	283	1,45	363	296	416	302	237	250	250	1,28	1,04	0,84	0,88		
					750	307	1,69	444	346	512	347	264	283	283	1,45	1,13	0,86	0,92		
	$b_w=114$	1150	830    105    863,5	284,2    262,7	150	147	0,73	150	139	139	139	139	139	139	1,02	0,95	0,95	0,95		
					250	229	0,94	216	197	221	199	180	197	197	0,94	0,86	0,78	0,86		
					350	290	1,11	270	241	295	242	207	241	241	0,93	0,83	0,71	0,83		
					550	323	1,39	364	308	421	305	246	308	308	1,13	0,95	0,76	0,95		
					750	343	1,62	444	360	521	351	275	277	277	1,30	1,05	0,80	0,81		
$b_w=120$	$b_w=106$	1150	710    105    801,0	238,6    261,1	150	143	0,79	150	133	139	139	133	133	133	1,05	0,93	0,93	0,93		
					250	190	1,02	216	184	219	197	168	184	184	1,13	0,97	0,89	0,97		
					350	232	1,21	270	223	292	239	192	223	223	1,16	0,96	0,83	0,96		
					550	271	1,52	363	283	413	301	227	246	246	1,34	1,04	0,84	0,91		
					750	289	1,77	443	330	507	344	253	280	280	1,53	1,14	0,88	0,97		

Table C2: C columns: SFEA ultimate strengths and corresponding DSM estimates (dimensions in  $mm$ , stresses in  $MPa$ ) – II

			GBT			SFEA			DSM											
		L	$L_{cr,D}$	$L_{cr,L}$	$f_E$	$f_D$	$f_L$	$f_y$	$f_U$	$\lambda_D$	$f_{NL}$	$f_{ND}$	$f_{NE}$	$f_{NLE}$	$f_{NDL}$	$f^{*}_{NDL}$	$\frac{f_{NL}}{f_U}$	$\frac{f_{ND}}{f_U}$	$\frac{f_{NDL}}{f_U}$	$\frac{f^{*}_{NDL}}{f_U}$
$b_w=100, b_s=10, t=2.4mm$	$b_l=55$	620	595	85	273,3	150	95	1,20	113	96	119	97	82	96	1,19	1,01	0,86	1,01		
						250	112	1,55	157	126	170	123	99	106	1,40	1,12	0,88	0,95		
						103,6	103,8	1,84	195	148	205	138	111	122	1,56	1,19	0,89	0,97		
						550	138	2,30	261	183	237	152	128	145	1,89	1,33	0,93	1,05		
						750	155	2,69	317	211	240	153	141	163	2,04	1,36	0,91	1,05		
$b_w=100, b_s=10, t=2.4mm$	$b_l=50$	620	590	85	240,4	150	95,4	1,19	117	97	116	98	84	97	1,22	1,02	0,88	1,02		
						250	116	1,53	163	127	162	123	102	109	1,40	1,10	0,88	0,94		
						106,7	114,6	1,81	202	151	190	136	114	125	1,62	1,20	0,92	1,00		
						550	135	2,27	270	186	211	146	133	149	2,00	1,38	0,98	1,11		
						750	152	2,65	329	215	211	146	146	168	2,16	1,41	0,96	1,11		
$b_w=100, b_s=10, t=1.9mm$	$b_l=60$	620	605	90	321,9	150	92,5	1,27	107	92	123	94	76	92	1,16	0,99	0,82	0,99		
						250	100	1,64	149	119	181	121	91	101	1,49	1,19	0,91	1,01		
						93,4	88,9	1,94	185	141	222	138	102	116	1,57	1,19	0,87	0,99		
						550	136	2,43	246	173	269	156	118	139	1,81	1,28	0,87	1,02		
						750	150	2,83	299	200	282	161	130	157	1,99	1,33	0,87	1,05		
$b_w=100, b_s=10, t=1.9mm$	$b_l=110$	1030	500	100	1725,3	150	126	0,94	133	118	145	130	110	118	1,06	0,94	0,87	0,94		
						250	166	1,21	187	159	235	180	135	159	1,13	0,96	0,82	0,96		
						170,8	171,6	1,43	233	191	322	221	153	182	1,24	1,01	0,81	0,96		
						550	221	1,79	313	239	481	287	180	226	1,41	1,08	0,81	1,02		
						750	254	2,10	381	277	625	339	199	260	1,50	1,09	0,78	1,02		
$b_w=100, b_s=10, t=1.9mm$	$b_l=130$	1030	505	100	1867,1	150	125	0,95	129	117	145	126	107	117	1,03	0,94	0,85	0,94		
						250	162	1,23	182	157	236	175	131	157	1,12	0,97	0,81	0,97		
						165,9	156,8	1,45	226	188	324	215	149	179	1,24	1,03	0,81	0,98		
						550	221	1,82	303	235	486	280	174	221	1,37	1,06	0,79	1,00		
						750	255	2,13	369	273	634	331	193	255	1,45	1,07	0,76	1,00		
$b_w=180, b_s=20, t=4.0mm$	$b_l=90$	1030	495	90	1537,3	150	128	0,92	139	120	144	135	114	120	1,08	0,94	0,89	0,94		
						250	172	1,19	195	162	234	187	141	162	1,14	0,94	0,82	0,94		
						177,0	194,0	1,41	244	194	318	229	160	182	1,23	0,98	0,81	0,92		
						550	207	1,76	327	243	474	297	187	224	1,58	1,18	0,90	1,08		
						750	260	2,06	399	282	611	350	207	257	1,53	1,09	0,80	0,99		
$b_w=180, b_s=20, t=4.0mm$	$b_l=100$	2000	620	150	1398,2	150	149	0,56	150	150	143	143	150	150	1,01	1,01	1,01	1,01		
						250	239	0,72	250	233	232	232	233	233	1,05	0,98	0,98	0,98		
						482,2	498,8	0,85	334	296	315	310	286	296	1,18	1,04	1,01	1,04		
						550	361	1,07	453	391	467	405	348	391	1,25	1,08	0,96	1,08		
						750	430	1,25	556	465	599	479	393	465	1,29	1,08	0,91	1,08		
$b_w=180, b_s=20, t=4.0mm$	$b_l=90$	2000	580	145	1335,3	150	149	0,53	150	150	143	143	150	150	1,01	1,01	1,01	1,01		
						250	245	0,69	250	238	231	231	238	238	1,02	0,97	0,97	0,97		
						526,3	504,8	0,82	335	304	314	311	295	304	1,10	1,00	0,97	1,00		
						550	377	1,02	454	405	463	405	361	405	1,21	1,07	0,96	1,07		
						750	442	1,19	558	484	593	478	409	484	1,26	1,09	0,92	1,09		
$b_w=180, b_s=20, t=4.0mm$	$b_l=110$	2000	660	150	1446,4	150	149	0,58	150	150	144	144	150	150	1,01	1,00	1,00	1,00		
						250	225	0,75	250	228	233	233	228	228	1,11	1,01	1,01	1,01		
						438,8	492,0	0,89	332	286	316	310	277	286	1,25	1,08	1,04	1,08		
						550	349	1,12	451	375	469	405	334	375	1,29	1,08	0,96	1,08		
						750	418	1,31	553	445	604	479	377	445	1,32	1,07	0,90	1,07		

Table C3: C columns: SFEA ultimate strengths and corresponding DSM estimates (dimensions in  $mm$ , stresses in  $MPa$ ) – III

		GBT			SFEA			DSM														
		L	$L_{cr,D}$	$L_{cr,L}$	$f_E$	$f_D$	$f_L$	$f_y$	$f_U$	$\lambda_D$	$f_{NL}$	$f_{ND}$	$f_{NE}$	$f_{NLE}$	$f_{NDL}$	$f^{*}_{NDL}$	$\frac{f_{NL}}{f_U}$	$\frac{f_{ND}}{f_U}$	$\frac{f_{NDL}}{f_U}$	$\frac{f^{*}_{NDL}}{f_U}$		
$b_w=110, b_s=85, t=2.4mm$	$b_s=15$	940	545	95	2702,1	457,5	457,4	350	304	150	148	0,57	150	150	147	147	150	150	1,01	1,01	1,01	1,01
										250	239	0,74	250	230	241	241	230	230	1,05	0,96	0,96	0,96
										550	398	0,87	325	290	332	313	276	290	1,07	0,96	0,91	0,96
										750	459	1,10	440	382	505	415	335	382	1,10	0,96	0,84	0,96
										1,28	540	454	668	500	378	454			1,18	0,99	0,82	0,99
	$b_s=13$	940	495	100	2606,7	379,7	454,7	350	287	150	148	0,63	150	148	146	146	148	148	1,01	1,00	1,00	1,00
										250	232	0,81	250	218	240	240	218	218	1,08	0,94	0,94	0,94
										550	380	0,96	324	271	331	312	258	271	1,13	0,94	0,90	0,94
										750	434	1,20	439	352	504	414	310	352	1,15	0,93	0,82	0,93
										1,41	539	416	665	498	348	401			1,24	0,96	0,80	0,92
$b_w=100, b_s=5, t=1.0mm$	$b_s=17$	940	595	95	2806,7	498,2	459,0	350	320	150	148	0,55	150	150	147	147	150	150	1,01	1,01	1,01	1,01
										250	243	0,71	250	235	241	241	235	235	1,03	0,97	0,97	0,97
										550	434	0,84	325	299	332	314	284	299	1,02	0,93	0,89	0,93
										750	491	1,05	440	396	507	417	346	396	1,01	0,91	0,80	0,91
										1,23	540	472	671	502	392	472			1,10	0,96	0,80	0,96
	$b_s=19$	1400	270	80	716,9	105,2	104,1	350	159	150	103	1,19	113	97	137	106	82	97	1,10	0,94	0,80	0,94
										250	133	1,54	157	127	216	143	99	127	1,18	0,95	0,75	0,95
										550	191	1,82	196	149	285	172	112	149	1,23	0,94	0,70	0,94
										750	197	2,29	261	185	399	213	129	185	1,37	0,97	0,68	0,97
										1,67	317	213	484	241	143	213			1,61	1,08	0,72	1,08
$b_w=100, b_s=5, t=1.0mm$	$b_s=45$	1400	250	80	665,2	116,6	105,2	350	168	150	108	1,13	113	101	136	106	86	101	1,05	0,94	0,80	0,94
										250	137	1,46	158	133	214	143	104	133	1,15	0,97	0,76	0,97
										550	205	1,73	196	158	281	170	117	158	1,17	0,94	0,70	0,94
										750	223	2,17	262	195	389	210	136	195	1,28	0,95	0,67	0,95
										150	108	2,54	318	225	468	236	150	225	1,43	1,01	0,67	1,01
	$b_s=29$	1400	290	85	759,2	95,0	102,8	350	155	150	98,8	1,26	112	92	138	106	79	92	1,14	0,93	0,80	0,93
										250	116	1,62	157	120	218	143	95	120	1,35	1,04	0,82	1,04
										550	189	1,92	195	142	289	172	106	142	1,26	0,91	0,68	0,91
										750	207	2,41	316	201	496	243	135	201	1,37	0,93	0,65	0,93
										150	109	2,81	316	201	496	243	135	201	1,53	0,97	0,65	0,97
$b_w=80, b_s=10, t=1.3mm$	$b_s=55$	2400	540	95	405,2	126,2	126,6	350	145	150	108	1,09	121	105	128	109	92	105	1,12	0,97	0,85	0,97
										250	134	1,41	169	138	193	142	112	128	1,26	1,03	0,84	0,96
										550	161	1,67	210	164	244	166	126	150	1,45	1,13	0,87	1,03
										750	176	2,09	280	204	312	195	147	183	1,74	1,27	0,91	1,13
										150	109	2,44	341	235	346	208	162	209	1,94	1,34	0,92	1,19
	$b_s=32$	2400	530	90	324,7	129,1	136,8	350	150	150	109	1,08	124	106	124	109	94	106	1,13	0,97	0,87	0,97
										250	138	1,39	173	140	181	140	115	140	1,26	1,01	0,83	1,01
										550	165	1,65	216	166	223	161	129	150	1,44	1,11	0,86	1,00
										750	179	2,06	288	206	271	182	151	183	1,75	1,25	0,91	1,11
										150	105	2,41	351	238	285	189	166	208	1,96	1,33	0,93	1,16
$b_w=125$	$b_s=100$	2400	545	105	459,4	119,9	109,0	350	140	150	105	1,12	115	102	131	105	87	102	1,09	0,98	0,83	0,98
										250	128	1,44	160	135	199	138	106	127	1,25	1,05	0,83	0,99
										550	160	1,71	199	160	254	162	120	149	1,42	1,14	0,85	1,07
										750	176	2,14	265	198	333	193	139	183	1,66	1,24	0,87	1,15
										150	105	2,50	323	229	379	209	154	210	1,83	1,30	0,87	1,19

Table C4: C columns: SFEA ultimate strengths and corresponding DSM estimates (dimensions in mm, stresses in MPa) – IV

			GBT			SFEA			DSM															
		L	L <sub>cr,D</sub>	L <sub>cr,L</sub>	f <sub>E</sub>	f <sub>D</sub>	f <sub>L</sub>	f <sub>y</sub>	f <sub>U</sub>	λ <sub>D</sub>	f <sub>NL</sub>	f <sub>ND</sub>	f <sub>NE</sub>	f <sub>NLE</sub>	f <sub>NDL</sub>	f <sup>*</sup> <sub>NDL</sub>	f <sub>NL</sub> / f <sub>U</sub>	f <sub>ND</sub> / f <sub>U</sub>	f <sub>NDL</sub> / f <sub>U</sub>	f <sup>*</sup> <sub>NDL</sub> / f <sub>U</sub>				
<i>b<sub>w</sub>=95, b=80, t=0.95mm</i>	<i>b<sub>s</sub>=10</i>	2500	610	85	273,0	94,1	93,8	350	111	150	91	1,26	109	92	119	94	77	92	1,20	1,01	0,85	1,01		
										250	106	1,63	152	120	170	118	93	99	1,43	1,13	0,87	0,93		
										193	188	141	205	133	104	113			1,70	1,27	0,93	1,02		
										550	130	2,42	251	174	237	147	120	134	1,93	1,34	0,92	1,03		
										750	145	2,82	305	200	239	148	132	150	2,10	1,38	0,91	1,03		
	<i>b<sub>s</sub>=9</i>	2500	570	85	268,3	87,8	93,5	350	106	150	87,7	1,31	109	89	119	93	75	89	1,24	1,02	0,85	1,02		
										250	99,8	1,69	152	116	169	118	90	99	1,52	1,16	0,90	0,99		
										550	130	2,00	188	136	203	132	100	113	1,78	1,28	0,95	1,07		
										750	146	2,50	251	168	233	145	116	136	1,93	1,29	0,89	1,04		
										2,92	305	193	235	146	127	153			2,09	1,32	0,87	1,05		
<i>b<sub>w</sub>=150, b<sub>s</sub>=10, t=1.2mm</i>	<i>b<sub>s</sub>=11</i>	2500	655	85	278,1	100,0	94,0	350	131	150	101	1,22	109	95	120	94	79	95	1,08	0,94	0,78	0,94		
										250	111	1,58	152	123	172	119	95	98	1,37	1,11	0,86	0,88		
										550	144	1,87	189	146	207	134	107	110	1,44	1,11	0,82	0,84		
										750	152	2,35	251	180	240	148	124	129	1,74	1,25	0,86	0,90		
										2,74	305	207	244	149	136	143			2,01	1,36	0,90	0,94		
	<i>b<sub>s</sub>=140</i>	1430	835	145	1969,7	54,1	53,7	350	97,1	150	60,6	1,67	90	70	145	88	54	64	1,48	1,16	0,89	1,05		
										250	79,8	2,15	124	90	237	120	64	80	1,56	1,13	0,80	1,00		
										550	123	2,54	154	105	325	147	71	92	1,58	1,08	0,73	0,95		
										750	145	3,19	204	128	489	190	82	111	1,66	1,04	0,66	0,90		
										2,72	248	147	640	224	89	126			1,71	1,01	0,62	0,87		
<i>b<sub>w</sub>=150, b<sub>s</sub>=10, t=1.2mm</i>	<i>b<sub>s</sub>=130</i>	1430	795	140	1949,9	59,8	57,4	350	99,6	150	63,5	1,58	92	74	145	90	57	68	1,44	1,16	0,90	1,06		
										250	83,1	2,04	127	95	237	123	68	85	1,53	1,14	0,82	1,02		
										550	127	2,42	157	111	325	150	76	98	1,58	1,11	0,76	0,98		
										750	149	3,03	209	136	489	194	87	119	1,65	1,07	0,69	0,93		
										2,54	248	147	638	230	95	135			1,70	1,04	0,64	0,90		
	<i>b<sub>s</sub>=140</i>	1430	870	155	1983,0	48,7	58,7	350	93,5	150	60,5	1,76	92	67	145	91	52	61	1,53	1,10	0,86	1,01		
										250	78,1	2,27	128	85	237	124	62	77	1,64	1,09	0,79	0,98		
										550	119	2,68	159	99	325	152	69	88	1,70	1,06	0,73	0,95		
										750	139	3,36	211	121	490	196	78	107	1,77	1,02	0,66	0,90		
										2,92	256	138	640	232	86	121			1,84	1,00	0,62	0,87		
<i>b<sub>w</sub>=200, b<sub>s</sub>=190, t=1.5mm</i>	<i>b<sub>s</sub>=125</i>	1850	1105	200	2304,3	46,1	46,1	350	89,4	150	57,5	1,80	85	65	146	83	49	59	1,48	1,13	0,85	1,03		
										250	75,5	2,33	117	82	239	114	57	74	1,56	1,09	0,76	0,98		
										550	114	3,45	193	117	498	181	73	103	1,69	1,03	0,64	0,91		
										750	133	4,03	234	134	654	215	80	118	1,76	1,01	0,60	0,88		
										2,56	233	120	646	212	72	98			1,58	1,00	0,70	0,86		
	<i>b<sub>s</sub>=145</i>	1850	1200	195	2104,5	38,1	45,6	350	88,2	150	55,3	1,98	84	59	146	83	44	52	1,53	1,06	0,80	0,93		
										250	74	2,56	117	74	238	113	52	64	1,64	0,98	0,65	0,83		
										550	112	3,03	145	86	326	138	58	73	1,71	0,94	0,59	0,78		
										750	132	3,80	192	105	493	179	66	87			1,76	0,91	0,55	0,75
										2,44	233	120	646	212	72	98			1,53	1,15	0,80	1,08		
<i>b<sub>s</sub>=11</i>	<i>b<sub>s</sub>=140</i>	1850	1010	205	2068,7	52,5	46,5	350	91,4	150	59	1,69	85	69	146	83	52	66	1,44	1,17	0,88	1,11		
										250	76,9	2,18	118	88	238	114	61	83	1,53	1,15	0,80	1,08		
										550	115	2,58	146	103	326	139	68	97	1,59	1,13	0,75	1,06		
										750	134	3,24	193	126	492	180	78	117	1,68	1,10	0,68	1,02		
										2,78	234	144	644	213	86	134			1,75	1,08	0,64	1,00		

Table C5: C columns: SFEA ultimate strengths and corresponding DSM estimates (dimensions in  $mm$ , stresses in  $MPa$ ) – V

			GBT			SFEA			DSM																		
		L	$L_{cr,D}$	$L_{cr,L}$	$f_E$	$f_D$	$f_L$	$f_y$	$f_U$	$\lambda_D$	$f_{NL}$	$f_{ND}$	$f_{NE}$	$f_{NLE}$	$f_{NDL}$	$f^{*}_{NDL}$	$\frac{f_{NL}}{f_U}$	$\frac{f_{ND}}{f_U}$	$\frac{f_{NDL}}{f_U}$	$\frac{f^{*}_{NDL}}{f_U}$							
$b_w=235, b_s=160, t=1.9mm$	$b_s=12.5$	1950	910	200	2378,7	64,4	64,4	150	74	1,53	96	77	146	94	61	75	1,29	1,04	0,82	1,01							
								250	94,4	1,97	133	99	239	129	72	95	1,41	1,04	0,76	1,01							
								550	144	2,33	164	115	329	158	80	111	1,47	1,03	0,72	0,99							
								750	169	3,41	265	162	657	244	101	156	1,52	0,98	0,64	0,94							
																	1,57	0,96	0,60	0,92							
$b_w=235, b_s=160, t=1.9mm$	$b_s=14$	1950	985	200	2401,8	55,7	64,1	150	72,9	1,64	95	71	146	94	57	68	1,31	0,98	0,78	0,94							
								250	91,6	2,12	132	91	239	129	67	86	1,45	1,00	0,73	0,94							
								550	142	3,14	218	130	500	205	86	122	1,49	0,97	0,68	0,91							
								750	168	3,67	265	149	658	244	94	139	1,54	0,92	0,60	0,86							
																	1,58	0,89	0,56	0,83							
$b_w=235, b_s=160, t=1.3mm$	$b_s=11$	1950	830	205	2357,0	74,0	64,6	150	76,9	1,42	96	82	146	94	64	82	1,24	1,07	0,84	1,07							
								250	97,4	1,84	133	106	239	129	77	106	1,36	1,09	0,79	1,08							
								550	143	2,17	164	124	329	158	86	124	1,46	1,10	0,76	1,10							
								750	167	2,73	219	153	499	206	99	152	1,53	1,07	0,69	1,06							
										3,18	265	175	656	244	109	175	1,59	1,05	0,65	1,05							
$b_w=150, b_s=10, t=1.3mm$	$b_s=140$	900	800	150	4970,4	63,5	63,5	150	70,9	1,54	95	76	148	94	60	71	1,34	1,07	0,85	1,01							
								250	94,4	1,98	132	98	245	130	71	90	1,40	1,04	0,76	0,95							
								550	145	2,35	163	114	340	160	80	104	1,45	1,01	0,70	0,92							
								750	170	2,94	217	140	525	211	91	127	1,50	0,97	0,63	0,87							
										3,44	264	161	704	254	100	144	1,55	0,95	0,59	0,85							
$b_w=150, b_s=10, t=1.3mm$	$b_s=130$	900	760	140	4920,3	71,4	67,8	150	75	1,45	97	81	148	96	64	75	1,30	1,08	0,85	1,00							
								250	99,6	1,87	135	104	245	133	76	95	1,36	1,04	0,77	0,96							
								550	152	2,21	167	122	340	164	85	111	1,41	1,02	0,72	0,93							
								750	178	2,78	223	150	525	216	98	134	1,46	0,98	0,65	0,88							
										3,24	270	172	704	260	108	153	1,52	0,96	0,61	0,86							
$b_w=150, b_s=10, t=1.3mm$	$b_s=140$	900	835	155	5004,5	58,2	58,2	150	67,2	1,61	92	73	148	91	57	68	1,37	1,09	0,84	1,01							
								250	87,6	2,07	128	93	245	126	67	86	1,46	1,07	0,77	0,98							
								550	138	2,45	158	109	340	155	75	99	1,47	1,01	0,69	0,92							
								750	163	3,07	210	134	525	204	86	120	1,52	0,97	0,62	0,87							
										3,59	255	153	704	245	94	137	1,57	0,94	0,58	0,84							
															<i>Mean</i>		1,37	1,04	0,82	0,97							
															<i>Sd.Dev.</i>		0,28	0,11	0,11	0,07							